# Description of the NIES FTIR observing system at Tsukuba, Japan: candidate for qualification as NDACC instrument

Isao Murata[1], Isamu Morino[2], and Hideaki Nakajima[2]

[1]Graduate School of Environmental Studies, Tohoku University

[2]National Institute for Environmental Studies (NIES)

FTIR measurements at National Institute for Environmental Studies (NIES), Tsukuba started in December 1998 with a Bruker 120M. The measurements with 120HR started in May 2001 and it was replaced by 125HR in April 2010. Here, the analyses for the measurements with 120HR and 125HR are described. The gas profiles and vertical column amounts are currently retrieved using SFIT4 v0.9.4.4 for default 10 species ($O_3$, $HNO_3$, HCl, HF, CO, $N_2O$, $CH_4$, HCN, $C_2H_6$, and $ClONO_2$) and others (HCHO, OCS, $NH_3$, $C_2H_2$, and $NO_2$).

*The official site report submitted to IRWG is attached at the last of this poster.

# Observational site and measurements

The Tsukuba site is in a suburban area (around 50 km from Tokyo) in a large plain with many rice paddies. The station occasionally captures local pollution and is affected by high humidity during the summer season.

Location: Tsukuba (36.05ºN, 140.1ºE, 31m A.S.L.)

Observation Period:

(120M: Dec. 1998 – Oct. 2006)

120HR: May 2001 – Mar. 2010 Filter 1-3 only

125HR: Apr. 2010 – Jan. 2014 Filter 1-4 only

Jan. 2014 – Filter 1-6

Observation Days: Around 50 (or more) days observation in a year

(more than 1200 days in total from 2001 to 2021)

# HBr cell measurement and ILS

HBr (#14) spectrum is recorded once a month.

The ILS was deduced by LINEFIT v.14. The 14 lines between 2412 $cm^{-1}$ and 2525 $cm^{-1}$ (between 2590 $cm^{-1}$ and 2675 $cm^{-1}$ before April 2013) were used.

The optical alignment has been good (no ILS correction needed) for 125HR since August 2011.

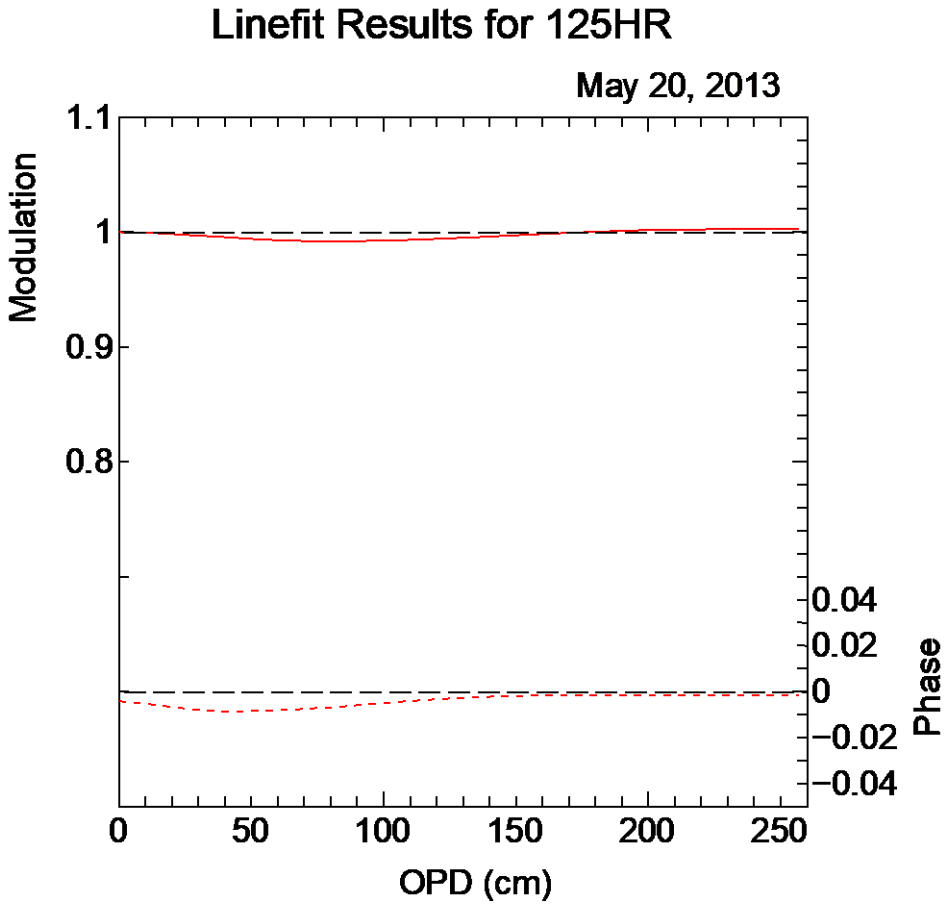

The ILS became worse due to the earthquakes in February 2005 (120HR) and March 2011 (125HR) and became better after the realignment.

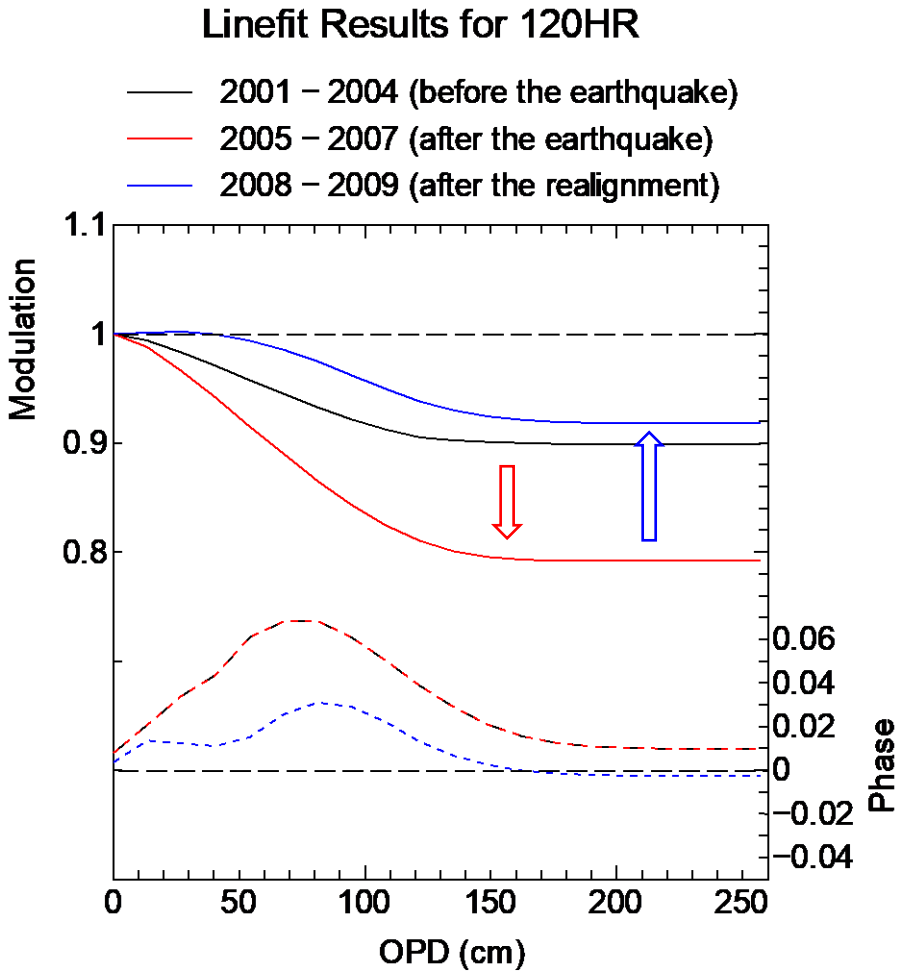


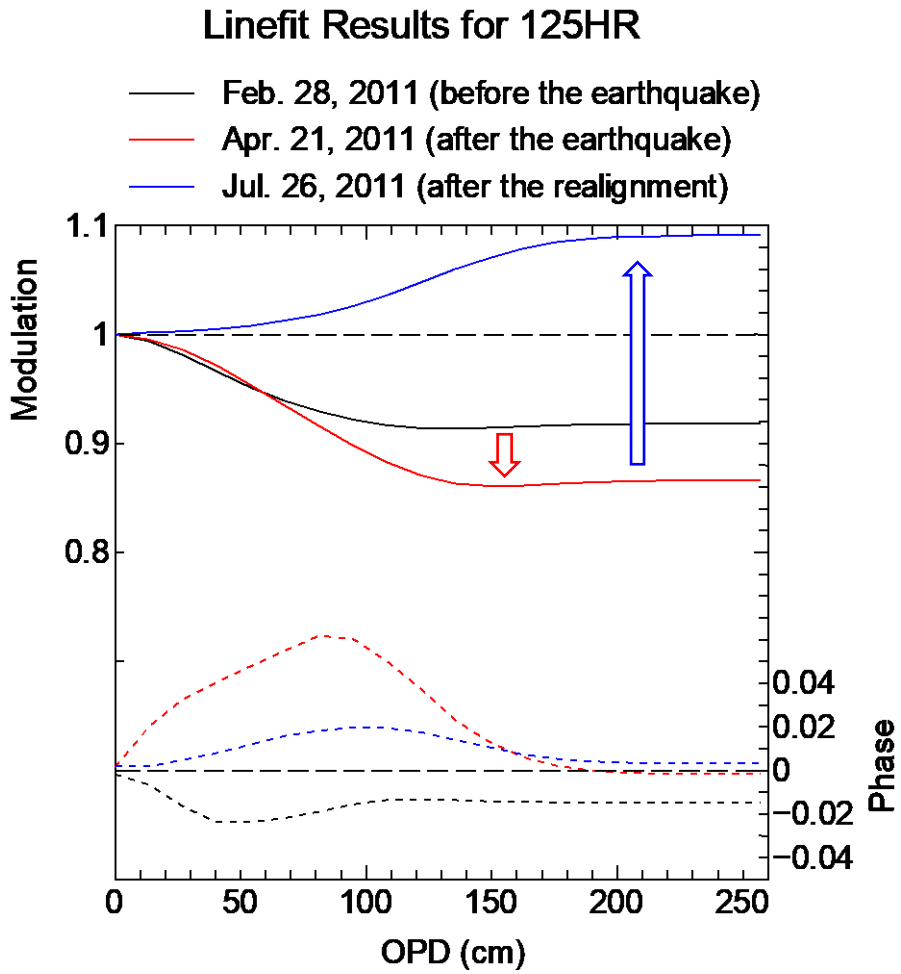

# Analysis

The gas profiles and vertical column amounts are currently retrieved using the inversion program SFIT4 v0.9.4.4.

## Measurement setting for filter #6 (MCT detector) and zero-level correction

Aperture size was changed twice:

### 0.8 mm (Jan. 24, 2014 – Jan. 4, 2017)

The observed spectra have almost no offset, but S/N was not enough for recoding small absorption feature.

### 1.15 mm (Jan. 10, 2017 – June 1, 2018)

There was still almost no offset, but more S/N were needed to retrieve the species with small absorptions like halocarbons.

### 1.7 mm (June 7, 2018 – present)

There is some offset and zero-level correction is needed, but S/N become much better.

# Results

## $O_3$

The retrieval for $O_3$ was performed using Vigouroux et al. [2008] and Vigouroux et al. [2015] as references. (See section 4.1 of the attached report for parameters and samples.)

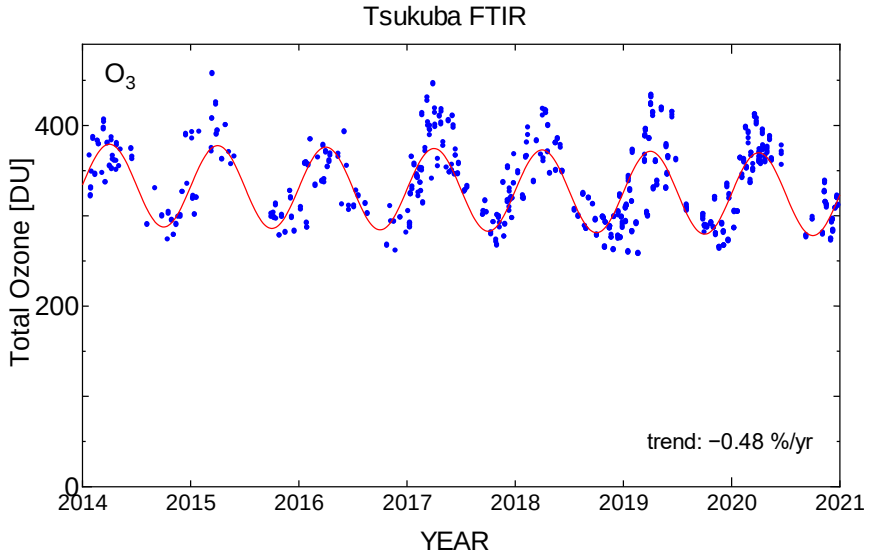


Fig. Temporal variation of total ozone.

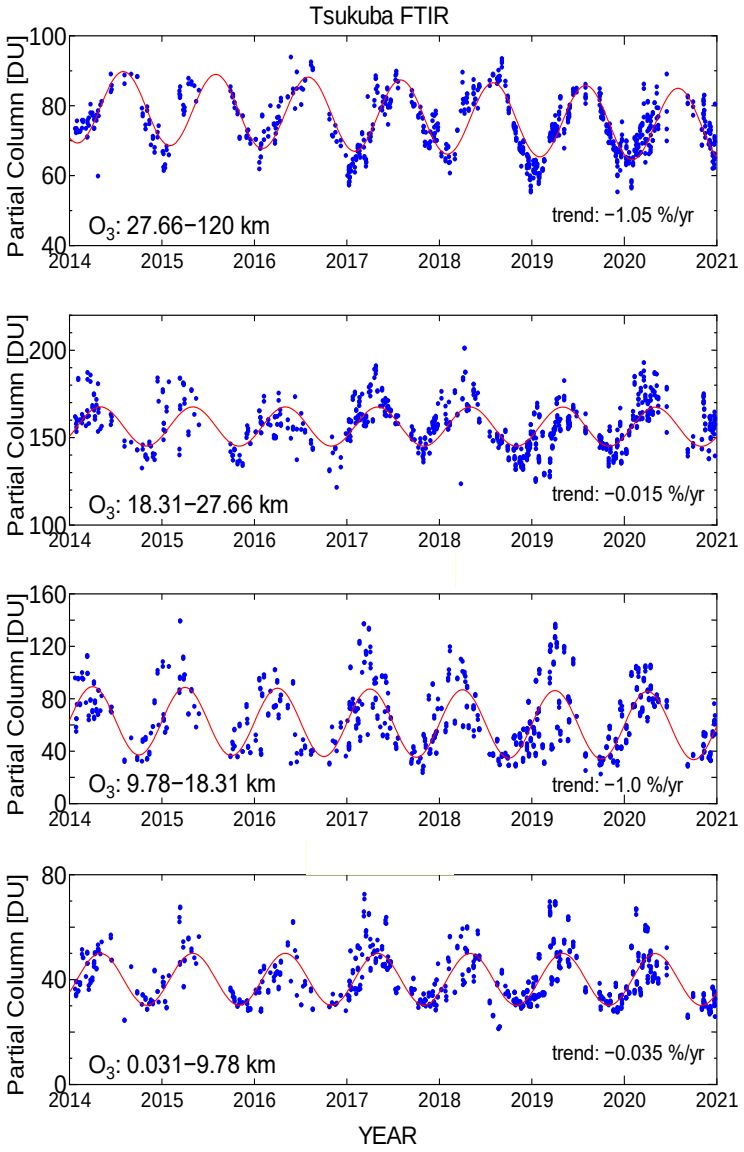


Fig. Temporal variation of partial columns of ozone.

## Validation for $O_3$ columns

Brewer and ozonesonde observations at Tateno on same days in 2019 were used.

### Total column

FTIR/Brewer ratio: 1.049 ± 0.24

This agrees with Vigouroux, et al. [2008]. The 5 % of bias may be due to the uncertainty of the line intensity.

### Partial column

FTIR/sonde ratio (15-days (58 spectra)):

1.03 ± 0.05 (18.3 - 27.7 km)

1.11 ± 0.19 (9.8 - 18.3 km)

1.02 ± 0.05 (0 - 9.8 km)

This indicates good agreement within ~10%.

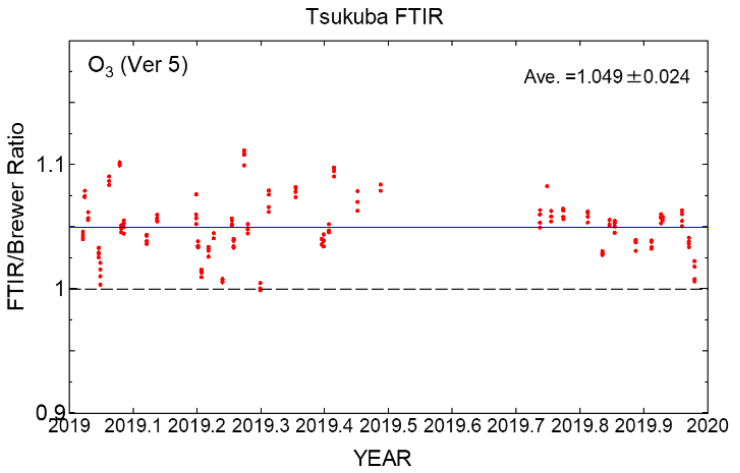


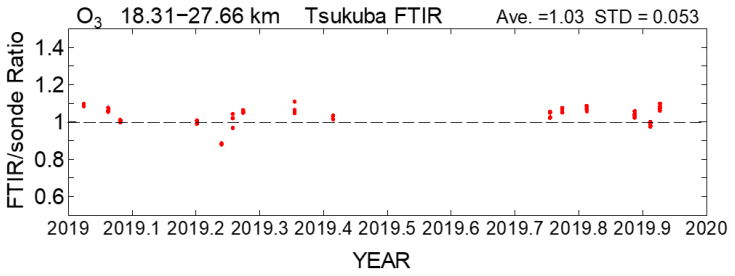


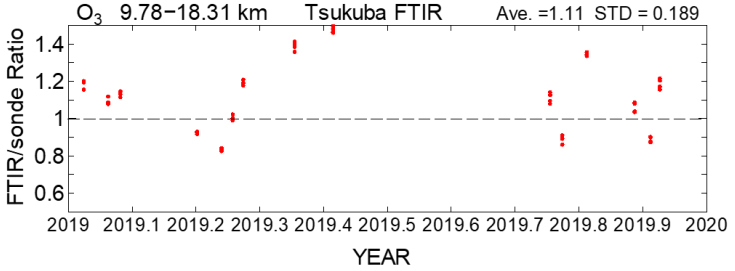


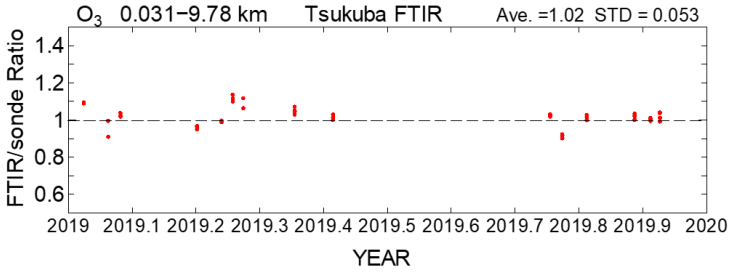

## $HNO_3$

The retrieval for $HNO_3$ was performed using one microwindow at 867.05 – 870.0 $cm^{-1}$. (See section 4.2 of the attached report for parameters and samples.)

The figure shows the temporal variation of vertical column of $HNO_3$. We can see the gap (10 % or more) at mid-2018 when aperture size was changed from 1.15 to 1.7. Because there is no saturated line in the microwindow for $HNO_3$ retrieval, we use optimized 2nd polynomial fit to fully absorbed regions in 10 μm region calculated in <pspec> (ZFlg=2) and no correction in <sfit4> for the spectra observed with the aperture size of 1.7 mm (after June 7, 2018).

We tested ZFlg=0 or 2 for all spectra but the differences in the retrieved columns were less than 2 %. This is consistent with the values of offset, and it means that the zero-level correction works well. We should investigate the reason for the gap…

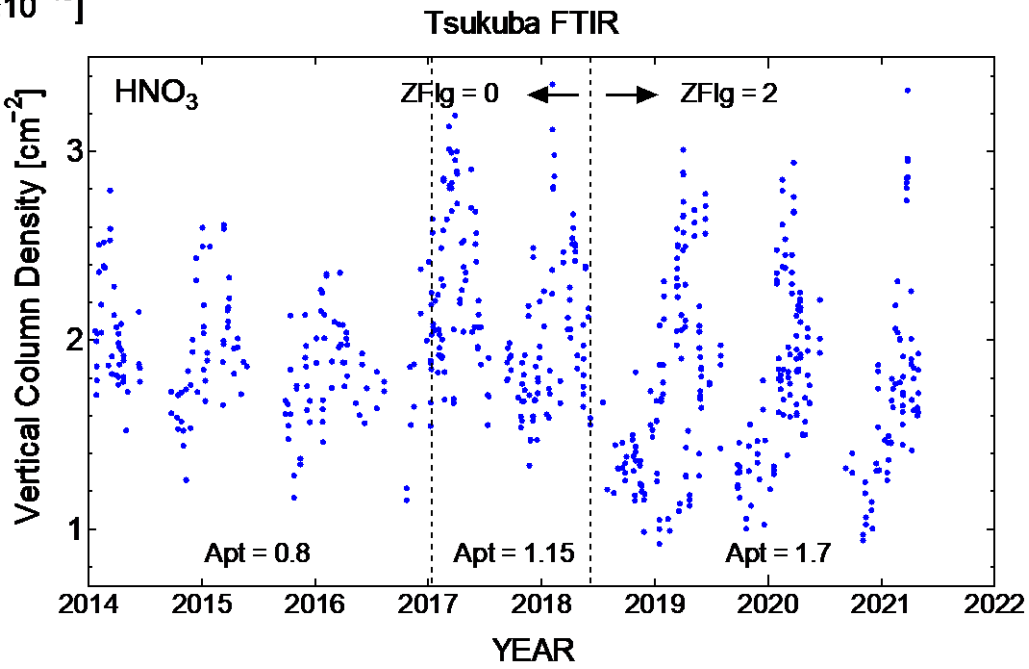


Fig. Temporal variation of vertical column of $HNO_3$.

## HCl

The retrieval for HCl was performed using 3 microwindows at 2727.73 – 2727.83, 2775.70 – 2775.80, and 2925.80 – 2926.00 $cm^{-1}$. (See section 4.3 of the attached report for parameters and samples.)

The figure shows the temporal variation of vertical column of HCl. We can see increasing and decreasing trends due to dynamical variation. Our results contributed to Kohlhepp et al. [2012] and Mahieu et al. [2014].

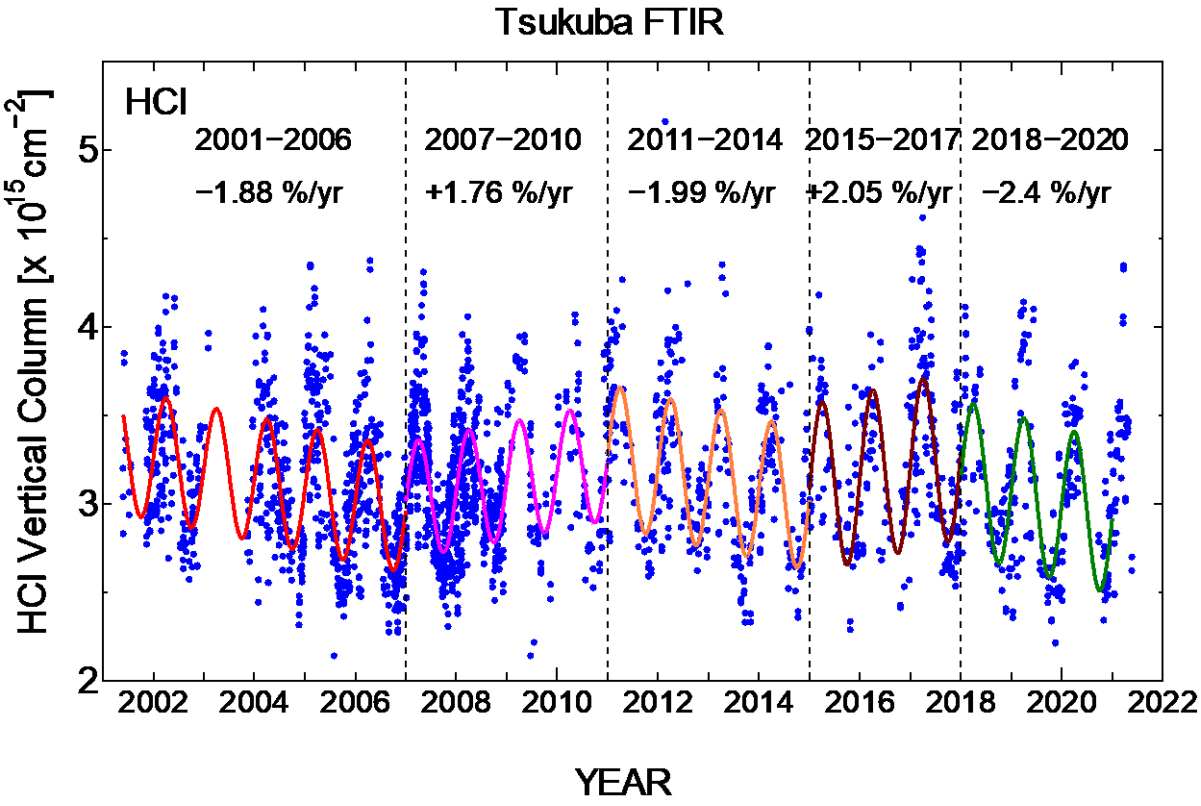


Fig. Temporal variation of vertical column of HCl.

## HF

The retrieval for HF was performed using one microwindow at 4038.81 – 4039.07 $cm^{-1}$. (See section 4.4 of the attached report for parameters and samples.)

The figure shows the temporal variation of vertical column of HF. We can see increasing and decreasing trends due to dynamical variation. Our results contributed to Kohlhepp et al. [2012].

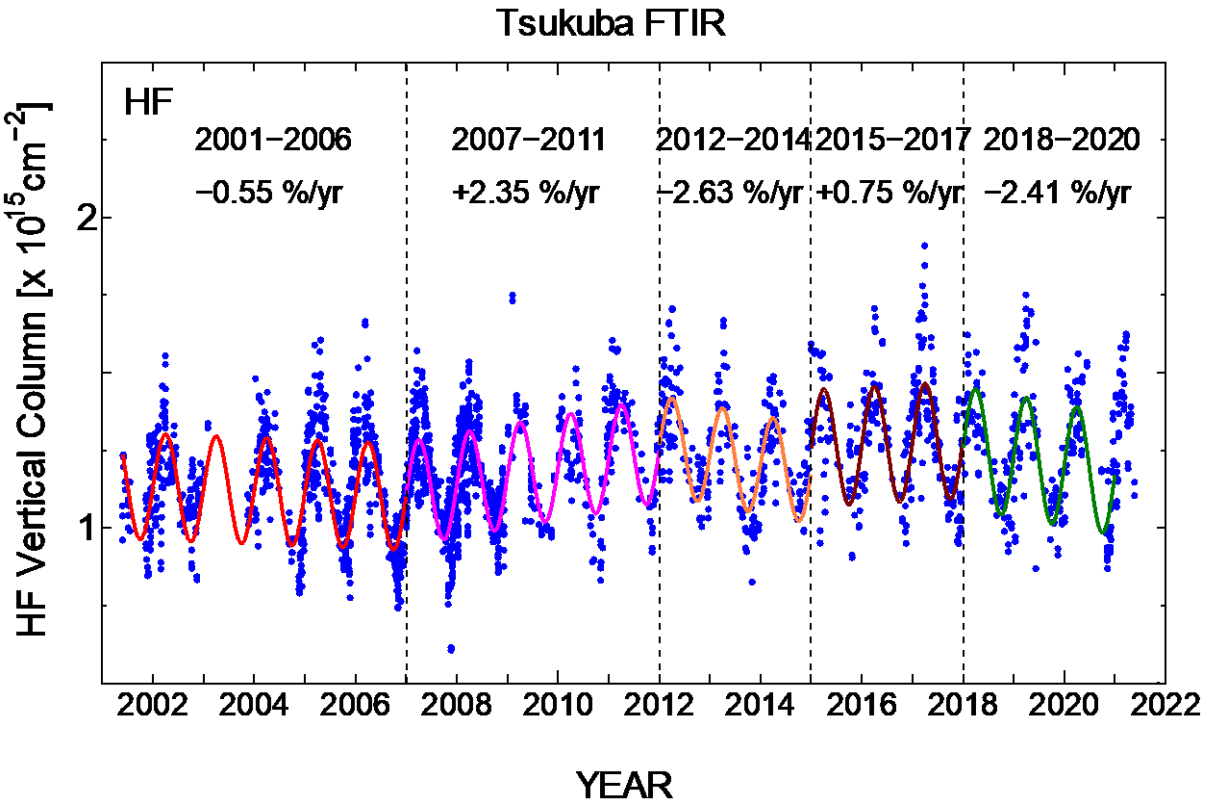


Fig. Temporal variation of vertical column of HF.

## CO

The retrieval for CO was performed using 3 microwindows at 2057.70 – 2058.00, 2069.56 – 2069.76, and 2157.50 – 2159.15 $cm^{-1}$. (See section 4.5 of the attached report for parameters and samples.)

The figure shows the temporal variation of vertical column of CO. We can see the decreasing trends.

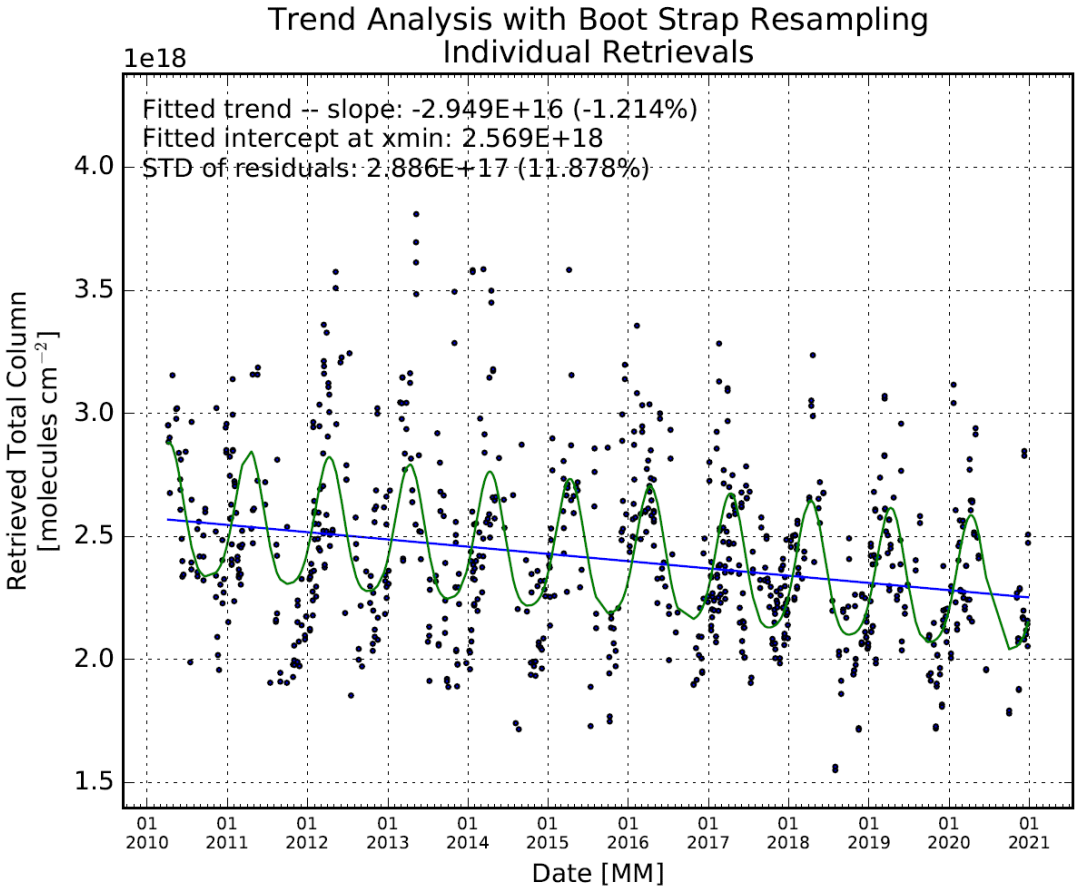


Fig. Temporal variation of vertical column of CO.

## $N_2O$

The retrieval for $N_2O$ was performed using 4 microwindows at 2481.30 – 2482.60, 2526.40 – 2528.20. 2537.85 – 2538.80, and 2540.10 – 2540.70 $cm^{-1}$. (See section 4.6 of the attached report for parameters and samples.)

The figure shows the temporal variation of vertical column of $N_2O$. The increasing trend between 2001 and 2021 is +0.22%/yr and that between 2010 and 2021 is +0.33%/yr, which is consistent with those reported in IPCC AR6 [2021].

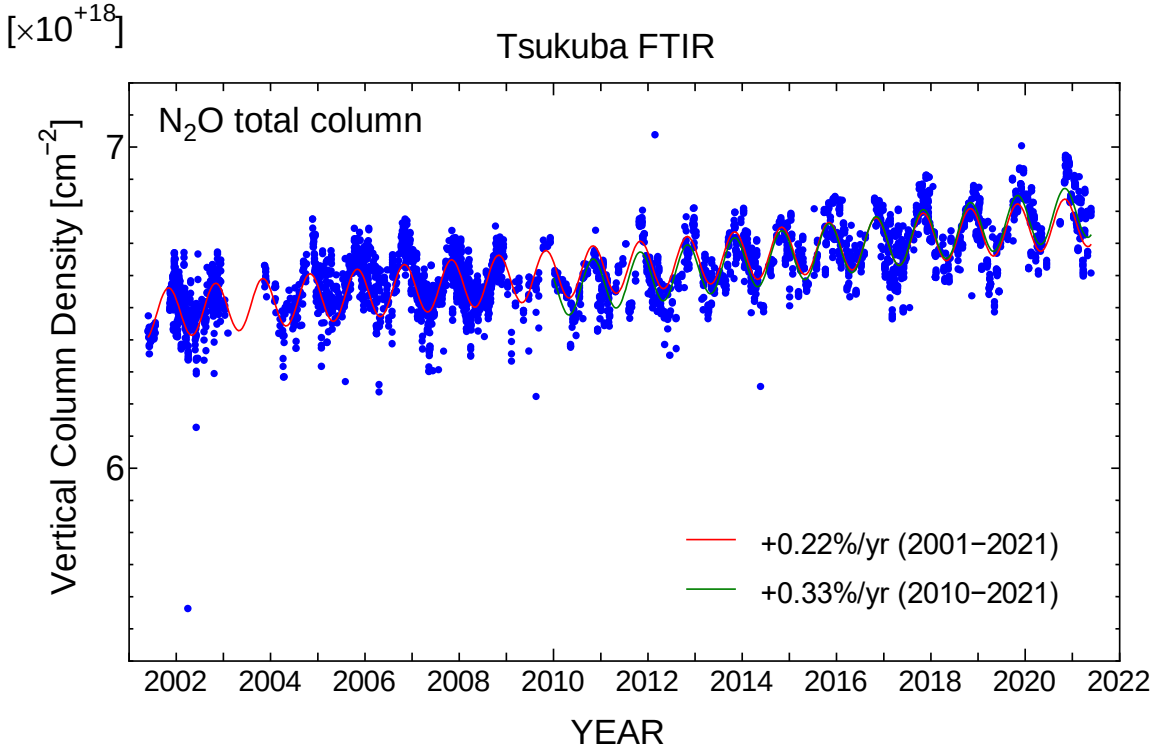


Fig. Temporal variation of vertical column of $N_2O$.

## $CH_4$

The retrieval for $CH_4$ was performed using Sussmann et al. [2011] as a reference. We use 3 microwindows at 2613.70 – 2615.40, 2835.50 – 2835.80, and 2921.00 – 2921.60 $cm^{-1}$. (See section 4.7 of the attached report for parameters and samples.)

We compared the retrieved tropospheric columns with airplane sampling results. FTIR/airplane ratio was 0.971 ± 0.017 when the retrieved results was limited by the RMS value of 0.15.

The figure shows the temporal variation of vertical column of $CH_4$. Our results contributed to Bader et al. [2017].

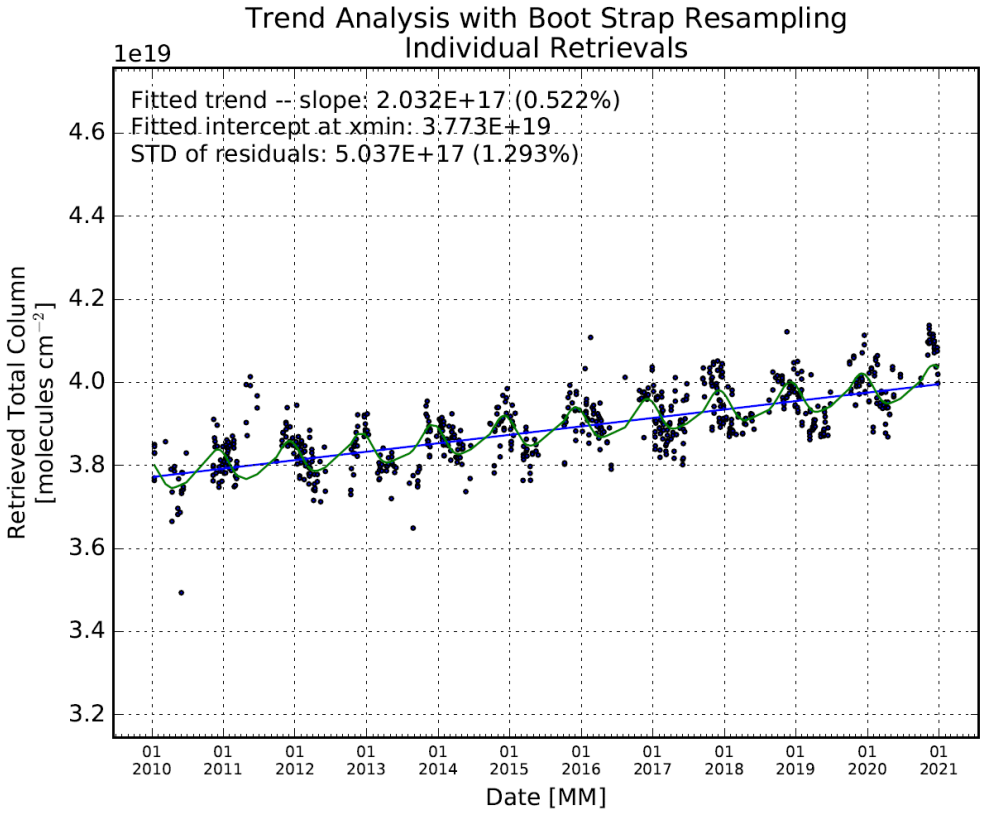


Fig. Temporal variation of vertical column of $CH_4$.

## HCN

The retrieval for HCN was performed using 3 microwindows at 3268.04 – 3268.40, 3287.10 – 3287.35, and 3299.40 – 3299.60 $cm^{-1}$. (See section 4.8 of the attached report for parameters and samples.)

The figure shows the temporal variation of vertical column of HCN.

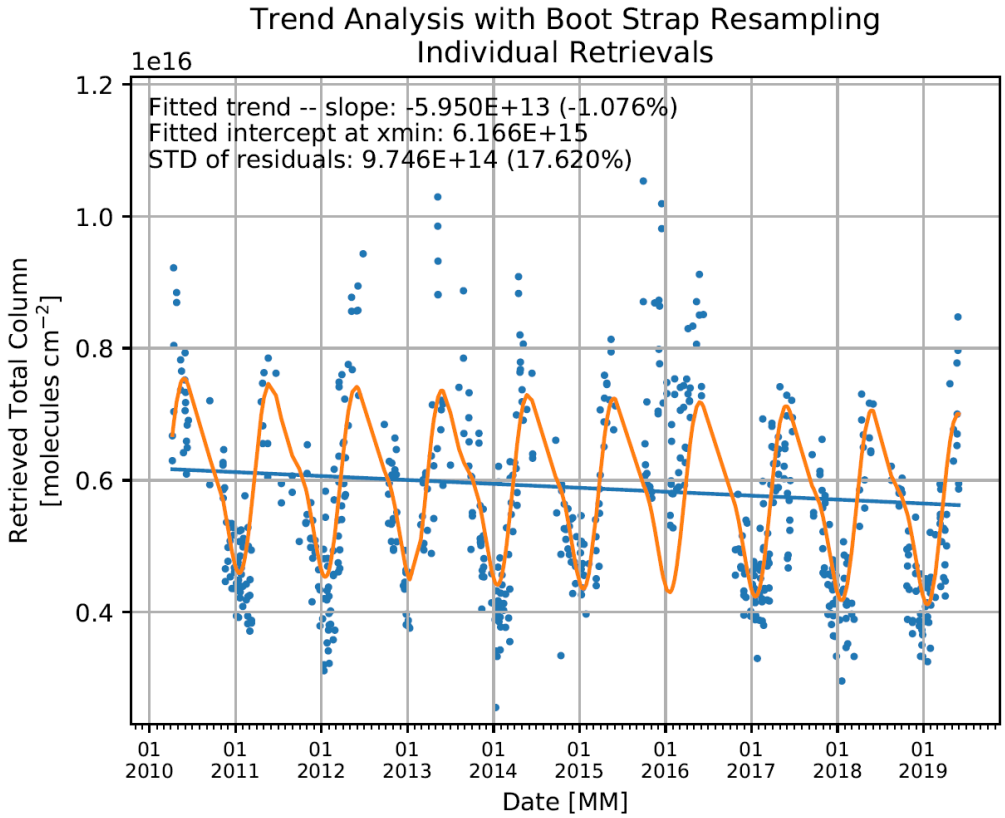


Fig. Temporal variation of vertical column of HCN.

## $C_2H_6$

The retrieval for $C_2H_6$ was performed using Franco et al. [2015] as a reference. We use 2 microwindows at 2976.660 – 2977.059 and 2983.200 – 2983.500 $cm^{-1}$. (See section 4.9 of the attached report for parameters and samples.)

The figure shows the temporal variation of vertical column of $C_2H_6$.

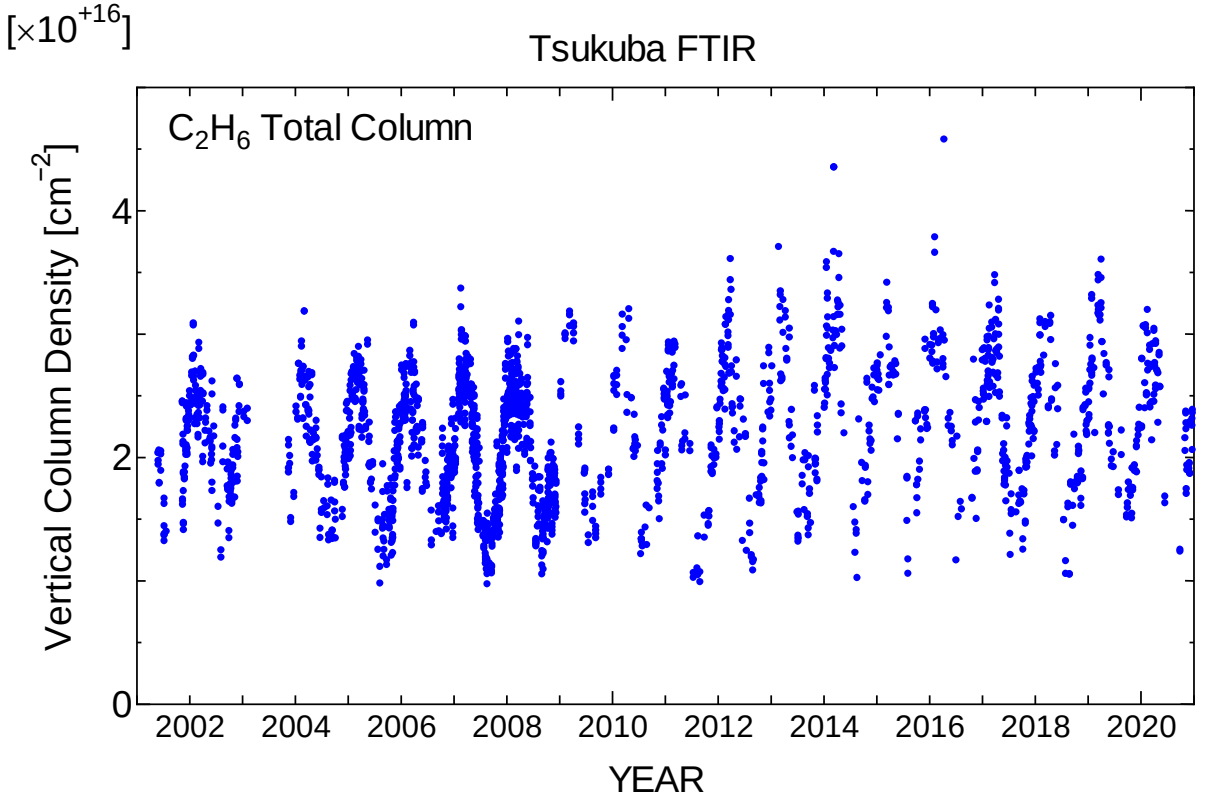


Fig. Temporal variation of vertical column of $C_2H_6$.

## $ClONO_2$

The retrieval for $ClONO_2$ was performed using parameters for Jungfraujoch (E. Mahieu, private communication) as a reference. We use one microwindow at 779.30 – 780.60 $cm^{-1}$. (See section 4.10 of the attached report for parameters and samples.)

The figure shows the temporal variation of vertical column of $ClONO_2$. Large day-to-day variation before mid-2018 is due to larger uncertainties come from smaller apertures.

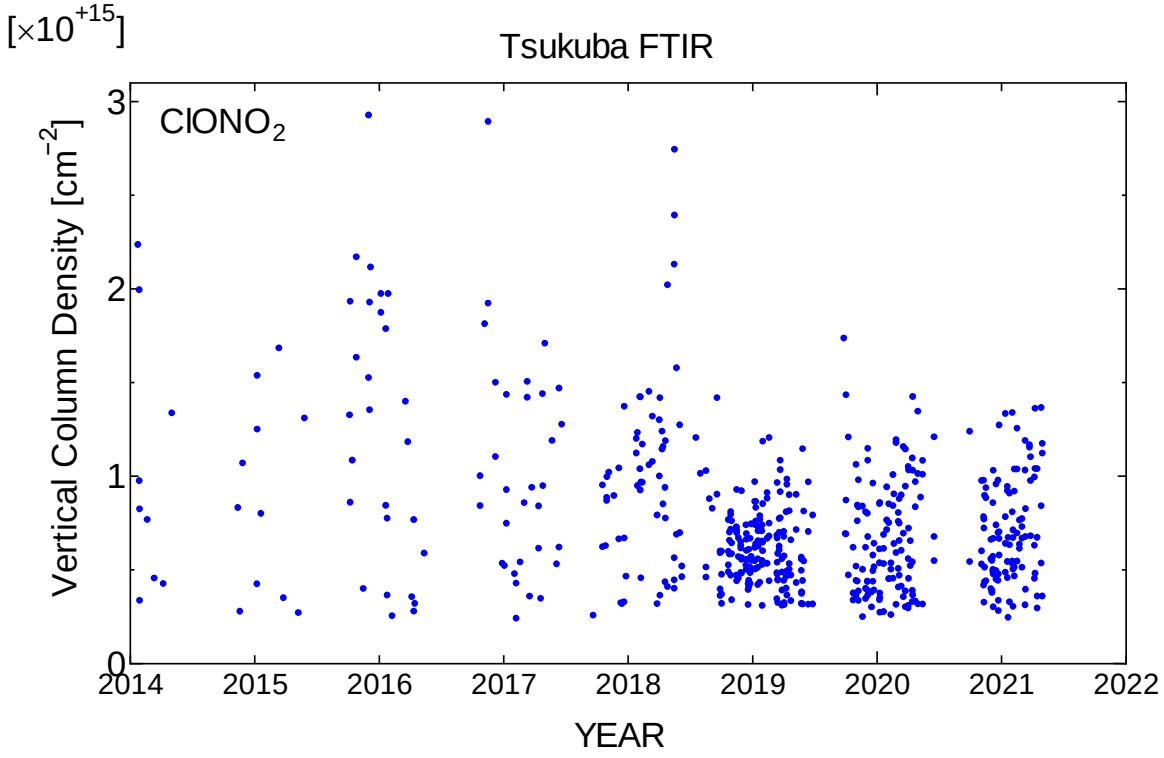


Fig. Temporal variation of vertical column of $ClONO_2$.

## HCHO

The retrieval for HCHO was performed using Vigouroux et al. [2018] as a reference. We use 4 microwindows at 2763.42 – 2764.17, 2765.65 – 2766.01, 2778.15 – 2779.10, and 2780.65 – 2782.00 $cm^{-1}$. (See section 4.11 of the attached report for parameters and samples.)

The figure shows the temporal variation of vertical column of HCHO. Our results contributed to Vigouroux et al. [2020].

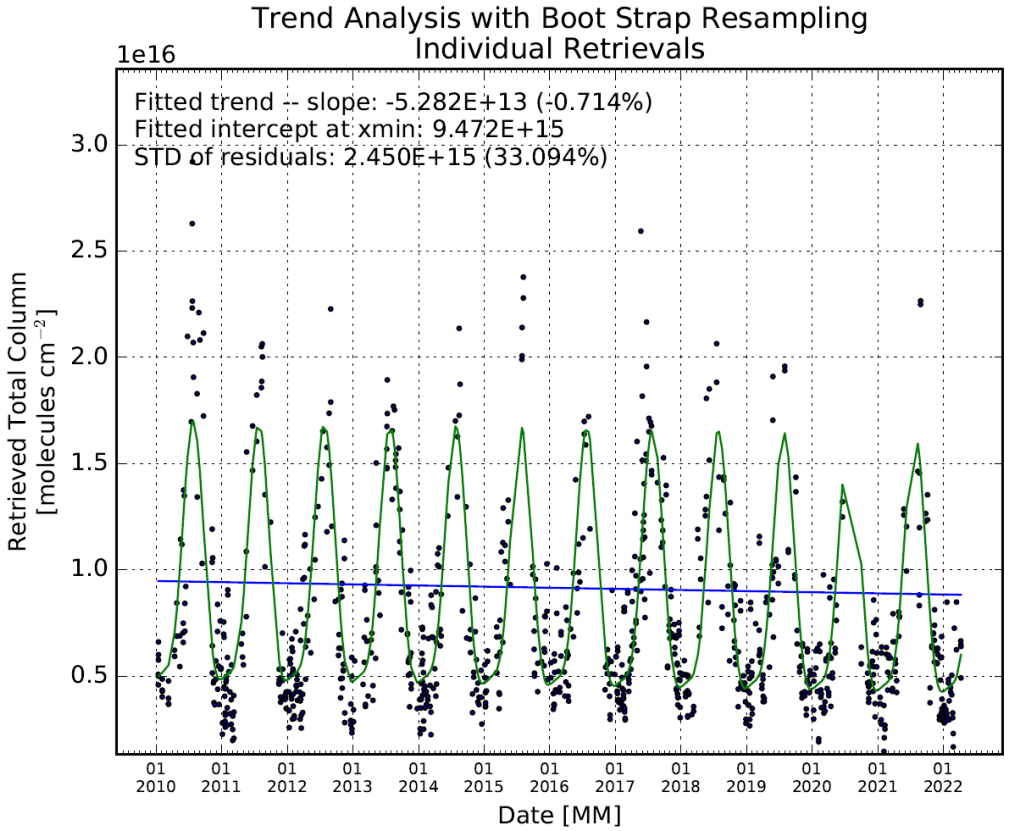


Fig. Temporal variation of vertical column of HCHO.

## OCS

The retrieval for OCS was described in Hannigan et al. [2022] in detail. We use 5 microwindows at 2030.75 – 2031.06, 2047.85 – 2048.24, 2049.77 – 2050.18, 2051.18 – 2051.46, and 2054.33 – 2054.67 $cm^{-1}$. (See section 4.12 of the attached report for parameters and samples.)

The figure shows the temporal variation of vertical column of OCS. Our results contributed to Hannigan et al. [2022].

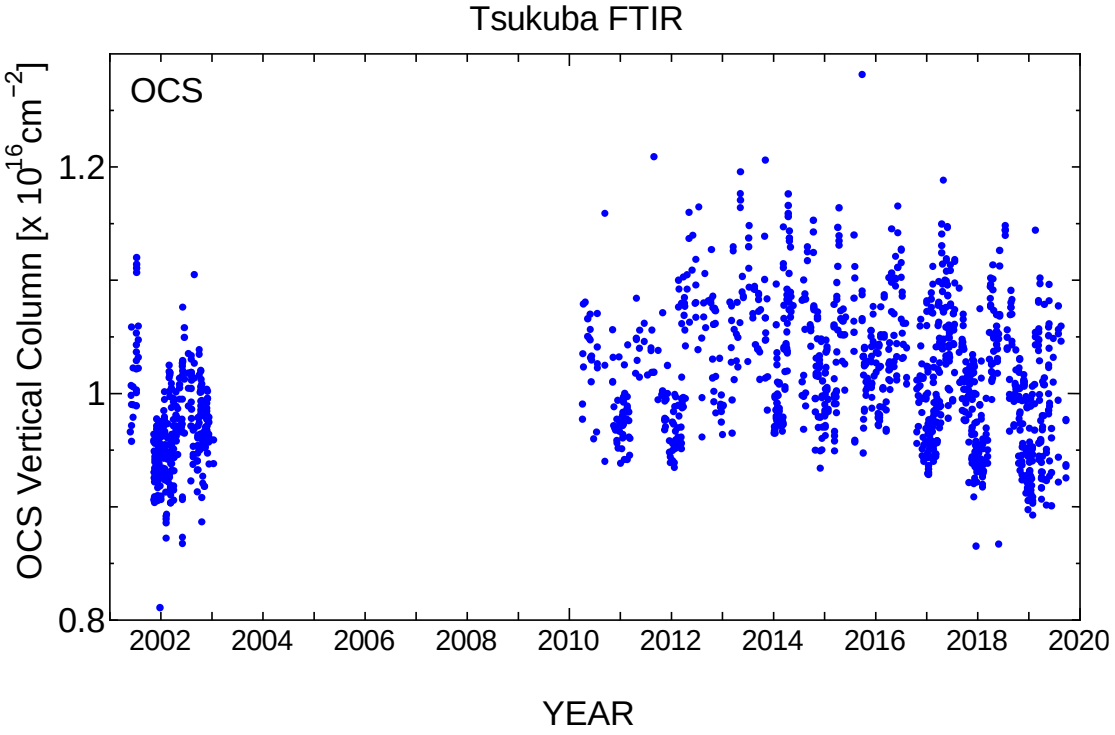


Fig. Temporal variation of vertical column of OCS.

## $NH_3$

The retrieval for $NH_3$ was performed using the parameters updated from Dammers et al. [2015]. We use 2 microwindows at 930.320 – 931.320 and 966.970 – 967.675 $cm^{-1}$. (See section 4.13 of the attached report for parameters and samples.)

The figure shows the temporal variation of vertical column of $NH_3$. Some high values maybe related to urban pollution or emission from agricultural land.

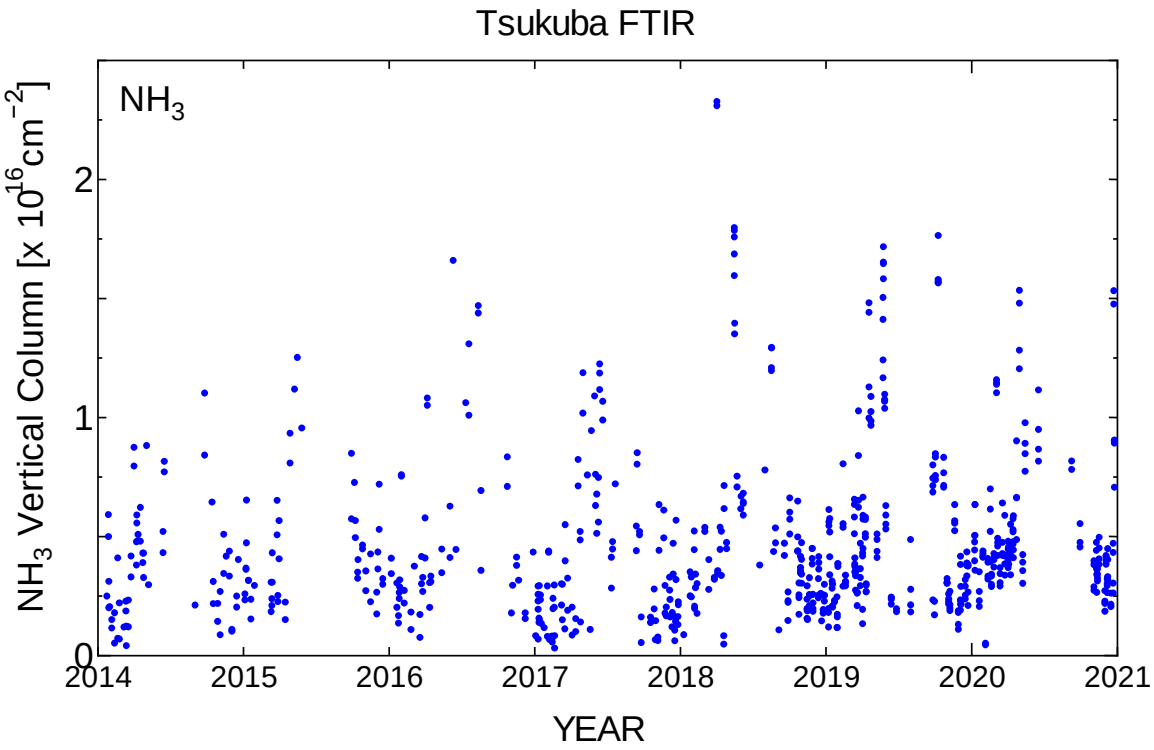


Fig. Temporal variation of vertical column of $NH_3$.

## $C_2H_2$

The retrieval for $C_2H_2$ was performed using one microwindow at 3250.25 – 3251.11 $cm^{-1}$. (See section 4.14 of the attached report for parameters and samples.)

The figure shows the temporal variation of vertical column of $C_2H_2$.

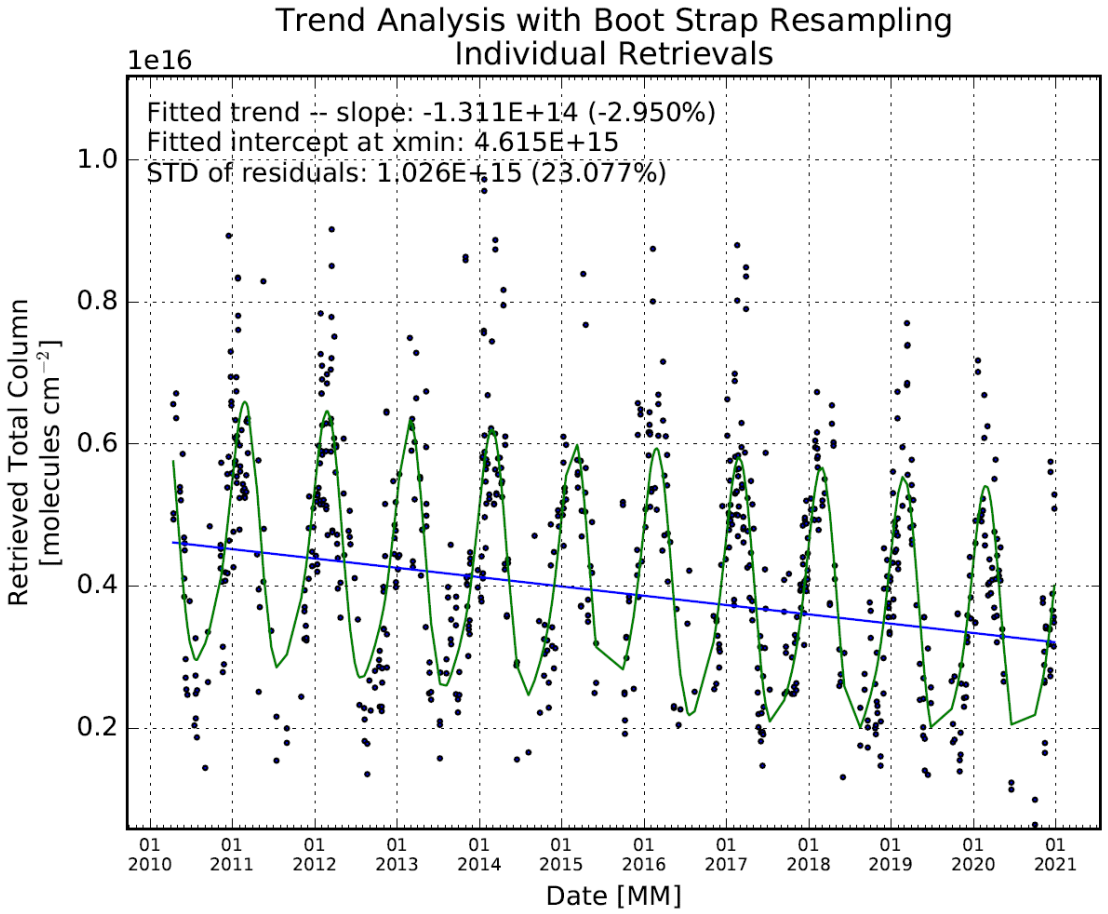


Fig. Temporal variation of vertical column of $C_2H_2$.

## $NO_2$

The retrieval for $NO_2$ was performed in corporation with C. Vigouroux. We use one microwindow at 2914.30 – 2914.85 $cm^{-1}$. (See section 4.15 of the attached report for parameters and samples.)

The figure shows the temporal variation of vertical column of $NO_2$.

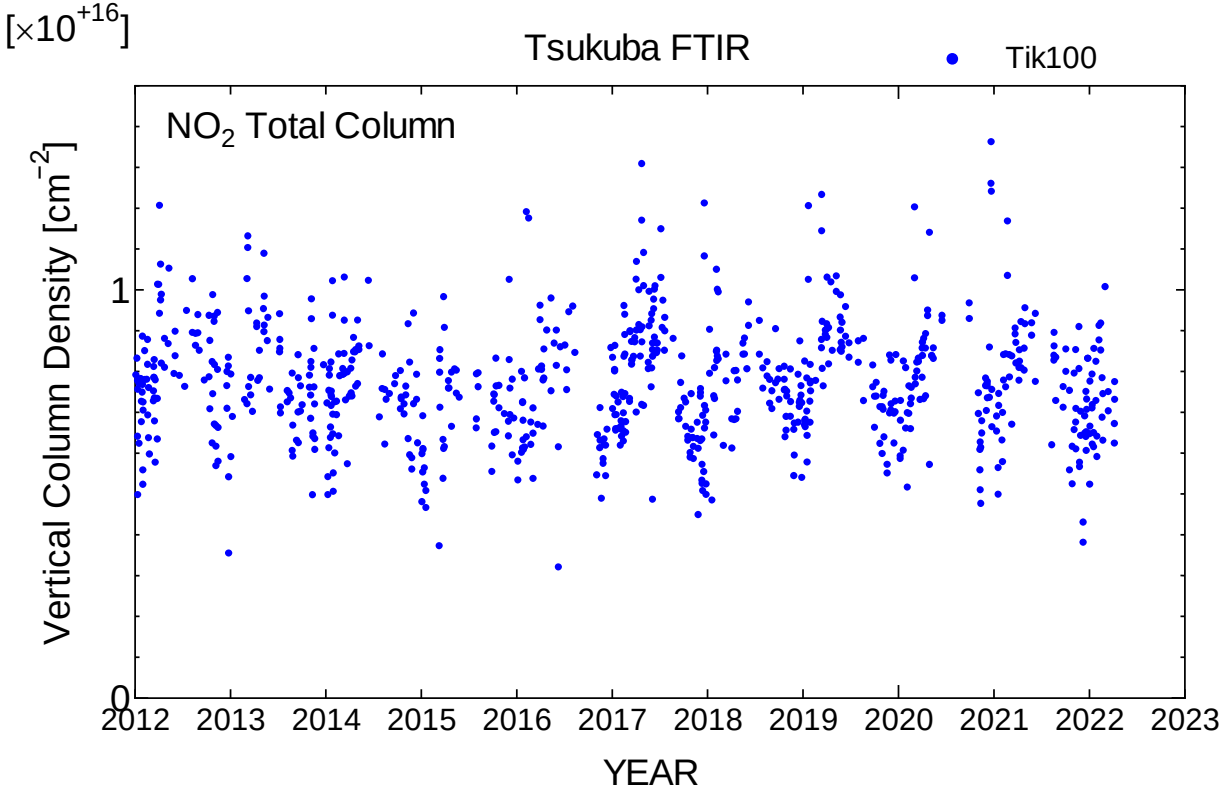


Fig. Temporal variation of vertical column of $NO_2$.

# Summary

The gas profiles and vertical column amounts observed at Tsukuba, Japan with 120HR and 125HR were retrieved using SFIT4 v0.9.4.4 for default 10 species ($O_3$, $HNO_3$, HCl, HF, CO, $N_2O$, $CH_4$, HCN, $C_2H_6$, and $ClONO_2$) and others (HCHO, OCS, $NH_3$, $C_2H_2$, and $NO_2$).

The results will be updated soon using SFIT4 v1.

The spectra observed with 120M will be analyzed later.

# Description of the NIES FTIR observing system at Tsukuba, Japan: candidate for qualification as NDACC instrument

Isamu Morino, Isao Murata, Hideaki Nakajima

June 8, 2022

**Participating institute(s)**
National Institute for Environmental Studies (NIES),
Onogawa 16-2, Tsukuba, Ibaraki 305-8506, Japan
Phone: +81-29-850-2515 / Fax: +81-29-850-2219
URL: http://www. nies.go.jp//
Graduate School of Environmental Studies, Tohoku University
Aramaki-Aoba, 6-3, Sendai, Miyagi, 980-8578, Japan
Phone: +81-22-795-5776
URL: http://www.kankyo.tohoku.ac.jp/

**Contact person(s)**
Dr. Isamu Morino, morino@nies.go.jp
Dr. Isao Murata, imurata@tohoku.ac.jp

# 1 Introduction

Fourier Transform Infra-Red (FTIR) measurements at National Institute for Environmental Studies (NIES), Tsukuba started in December 1998 with a Bruker 120M FTIR installed in the container and a Denver University solar tracker. The NDACC measurements with 120M had continued till October 2006, then it was moved to Syowa station, Antarctica. The measurements with 120HR in the observation room of the Climate Change Research Hall at NIES and original solar tracker started in May 2001. This was used mainly for near infra-red measurements (TCCON) but NDACC measurements with filter #1 – 3 were also performed. The 120HR was replaced by 125HR in April 2010 and NDACC measurements with filter #1 – 4 started. The measurements with filter #5 – 6 started in January 2014.

Here, the analyses for the measurements with 120HR and 125HR are described. Although we have 8 years measurements by 120M, unfortunately the optical alignment of our 120M was not so good and the correction of the spectra with instrumental line shape (ILS) observed by HBr and $N_2O$ cells has not finished yet. We will perform the correction and analysis for 120M measurements later.

# 2 Characteristics and parameters of the observing system

2.1 Instrument characteristics

The spectrometer is a Bruker IFS 125HR (120HR before March 2010). It is installed in an air-conditioned room and is equipped with an original solar tracker on the top of the building. The measurements are performed by an operator in the clear sky before or after TCCON measurements.

In order to monitor the alignment of the FTIR instrument, a reference gas cell containing hydrogen bromide (HBr) at 2 mbar (#14) was placed in the interferometer output beam in front of the indium antimonide (InSb) detector for 120HR and now is placed in the sample compartment for 125HR. HBr spectrum is recorded once a month using a MIR lamp as light source. The ILS was deduced from the gas cell HBr spectra using the LINEFIT v.14 software package.

The ILS became worse due to the earthquakes in February 2005 (120HR) and March 2011 (125HR). The optical alignment has been good (no ILS correction needed) since August 2011 after the realignment by the Bruker engineer (Gregor Surawicz).

2.2 Instrument parameters

| | **IFS 120HR** | **IFS 125HR** |
|---|---|---|
| **Maximum OPD** | 474 cm | 474 cm |
| **Maximum resolution** | 0.0019 $cm^{-1}$ | 0.0019 $cm^{-1}$ |
| **Aperture range** | 0.5 – 1.3 mm | 0.5 – 2.5 mm |
| **Time needed for 1 scan** | 100 s | 50 – 100 s |
| **Number of scans** | 2 (forward or backward) | 4 – 8 (forward + backward) |
| **Spectral range** | 2400 – 4400 $cm^{-1}$* | 500 – 4400 $cm^{-1}$ |

OPD = Optical Path Difference

*Only InSb detector was used for the NDACC measurements.

2.3 Optics features

| | | IFS 120HR | | IFS 125HR | |
|---|---|---|---|---|---|
| | | **> 50% transmission range ($cm^{-1}$)** | **> 0% transmission range ($cm^{-1}$)** | **> 50% transmission range ($cm^{-1}$)** | **> 0% transmission range ($cm^{-1}$)** |
| **Beam splitters** | $CaF_2$ | | 1850 – 11000 | | 1850 – 11000 |
| | KBr | | 450 – 4800 | | 450 – 4800 |
| **Optical bandpass filter** | NDACC #1 | 4065 – 4270 | 3850 – 4500 | 4065 – 4290 | 3850 – 4500 |
| | NDACC #2 | 3060 – 3800 | 2500 – 4200 | 3070 – 3800 | 2500 – 4200 |
| | NDACC #3 | 2450 – 3075 | 2220 – 3600 | 2400 – 3100 | 2220 – 3600 |
| | NDACC #4 | | | 2020 – 2570 | 1820 – 2860 |
| | NDACC #5 | | | 1860 – 2100 | 1600 – 2420 |
| | NDACC #6 | | | 846 – 1350 | 500 – 1480 |
| **Detectors** | InSb | | 1850 – 9600 | | 1850 – 9600 |
| | HgCdTe (MCT) | | | | 600 – 6000 |

MCT = Mercury Cadmium Telluride

2.4 Measurement configuration details

| Setting name | Resolution ($cm^{-1}$) | Single scan time (s) | Number of scans | Spectral range ($cm^{-1}$) | Beam splitter | Filter | Aperture (mm) | Detector |
|---|---|---|---|---|---|---|---|---|
| | | | | 120HR | | | | |
| 1M | 0.0035 | 100 | 2 | 3900 – 4400 | KBr/$CaF_2$* | NDACC #1 | 0.5 | InSb |
| 2M | 0.0035 | 100 | 2 | 2800 – 3700 | KBr/$CaF_2$* | NDACC #2 | 0.5 | InSb |
| 3M | 0.0035 | 100 | 2 | 2400 – 3200 | KBr/$CaF_2$* | NDACC #3 | 0.5 | InSb |
| HBr | 0.0035 | 100 | 32 | 2400 – 2894 | KBr/$CaF_2$* | NDACC #3 | 1.3 | InSb |
| BG** | 10.0 | 0.04 | 32 | 2400 – 2894 | KBr/$CaF_2$* | NDACC #3 | 1.3 | InSb |
| | | | | 125HR | | | | |
| 1M | 0.0035 | 100 | 4 | 3900 – 4400 | $CaF_2$ | NDACC #1 | 0.5 | InSb |
| 2M | 0.0035 | 100 | 4 | 2800 – 3700 | $CaF_2$ | NDACC #2 | 0.5 | InSb |
| 3M | 0.0035 | 100 | 4 | 2400 – 3200 | $CaF_2$ | NDACC #3 | 0.5 | InSb |
| 4M | 0.0035 | 100 | 4 | 1900 – 2800 | $CaF_2$ | NDACC #4 | 0.5 | InSb |
| 5M | 0.0035 | 100 | 4 | 1700 – 2200 | KBr | NDACC #5 | 0.5 | InSb |
| 6M | 0.0035 | 100 | 4 | 500 – 1380 | KBr | NDACC #6 | 0.8*** | MCT |
| | | | | | | | 1.15 | |
| | | | | | | | 1.7 | |
| 6L | 0.0070 | 50 | 8 | 500 – 1380 | KBr | NDACC #6 | 2.5 | MCT |
| HBr | 0.0035 | 100 | 64 | 2400 – 3200 | $CaF_2$ | NDACC #4 | 1.0 | InSb |
| BG** | 0.035 | 10 | 64 | 2400 – 3200 | $CaF_2$ | NDACC #4 | 1.0 | InSb |

*KBr was used for the measurements before March 2004. $CaF_2$ was used for the measurements after April 2004.

**BG setting is for the background measurements for the HBr cell measurements to calculate transmittance spectra.

***Aperture size for 6M was changed twice: 0.8 mm (Jan. 24, 2014 – Jan. 4, 2017)
1.15 mm (Jan. 10, 2017 – June 1, 2018)
1.7 mm (June 7, 2018 – present)

# 3 Characteristics of the observing site

The Tsukuba site is located in a suburban area (around 50 km from Tokyo) in a large plain with many rice paddies, at an altitude of 31 m. The station occasionally captures local pollution and is affected by high humidity during the summer season.

| Tsukuba site | |
|---|---|
| Latitude | 36.05°N |
| Longitude | 140.12°E |
| Altitude | 31 m a.s.l. |

The numbers of observing days per month for the period of 2001 – 2021 are given in the following table. Generally, the numbers are small in summer wet season (June to September) and the qualities of the spectra are not so good due to high humidity. Although the numbers of observing days per year (last column) varies especially before 2009, they are in the range of 40 to 50 days after 2010.

| **Year** | Jan. | Feb. | Mar. | Apr. | May | Jun. | Jul. | Aug. | Sep. | Oct. | Nov. | Dec. | **Total (yearly)** |
|---|---|---|---|---|---|---|---|---|---|---|---|---|---|
| **2001** | - | - | - | - | 2 | 5 | 6 | 0 | 0 | 0 | 7 | 12 | **32** |
| **2002** | 10 | 6 | 9 | 7 | 5 | 5 | 1 | 7 | 3 | 10 | 6 | 3 | **72** |
| **2003** | 1 | 1 | 0 | 0 | 0 | 0 | 0 | 0 | 0 | 0 | 3 | 3 | **8** |
| **2004** | 4 | 7 | 8 | 10 | 6 | 7 | 15 | 10 | 6 | 4 | 3 | 11 | **91** |
| **2005** | 10 | 9 | 9 | 11 | 4 | 4 | 7 | 8 | 9 | 7 | 15 | 12 | **105** |
| **2006** | 11 | 8 | 12 | 9 | 5 | 5 | 4 | 9 | 6 | 9 | 15 | 8 | **101** |
| **2007** | 6 | 12 | 13 | 6 | 14 | 13 | 5 | 12 | 8 | 10 | 14 | 13 | **126** |
| **2008** | 15 | 16 | 11 | 8 | 10 | 3 | 5 | 7 | 8 | 9 | 10 | 6 | **108** |
| **2009** | 1 | 1 | 1 | 1 | 2 | 5 | 1 | 2 | 1 | 1 | 1 | 1 | **18** |
| **2010** | 2 | 2 | 1 | 4 | 4 | 6 | 5 | 4 | 3 | 0 | 7 | 7 | **45** |
| **2011** | 8 | 8 | 4 | 3 | 3 | 1 | 1 | 5 | 3 | 1 | 6 | 4 | **47** |
| **2012** | 10 | 8 | 7 | 5 | 3 | 4 | 2 | 4 | 2 | 4 | 5 | 5 | **59** |
| **2013** | 2 | 1 | 6 | 3 | 6 | 0 | 4 | 5 | 4 | 2 | 8 | 1 | **42** |
| **2014** | 11 | 4 | 5 | 7 | 3 | 2 | 2 | 3 | 3 | 3 | 4 | 4 | **51** |
| **2015** | 6 | 1 | 6 | 4 | 3 | 1 | 3 | 1 | 1 | 5 | 2 | 5 | **38** |
| **2016** | 5 | 4 | 5 | 4 | 2 | 3 | 3 | 2 | 0 | 2 | 6 | 4 | **40** |
| **2017** | 7 | 9 | 7 | 6 | 5 | 7 | 5 | 2 | 4 | 6 | 5 | 10 | **73** |
| **2018** | 4 | 4 | 3 | 7 | 2 | 2 | 2 | 4 | 3 | 4 | 6 | 6 | **47** |
| **2019** | 8 | 4 | 6 | 6 | 5 | 2 | 1 | 2 | 2 | 3 | 5 | 5 | **49** |
| **2020** | 4 | 5 | 5 | 7 | 2 | 1 | 0 | 0 | 2 | 0 | 5 | 8 | **39** |
| **2021** | 4 | 6 | 4 | 5 | 1 | | | | | | | | |
| **Total (monthly)** | 129 | 116 | 122 | 113 | 87 | 76 | 72 | 87 | 68 | 80 | 133 | 128 | **1211** |

# 4 Observational data

The gas profiles and vertical column amounts are currently retrieved using the inversion program SFIT4 v0.9.4.4 (SFIT4 v1 is already installed and we are preparing to reanalyze all spectra).

| **Common settings** | |
|---|---|
| **Altitude grid** | 48 layers |
| **Spectroscopy*** | HITRAN2008 or ATM2016 |
| **Pressure and temperature profiles** | NCEP |
| **A priori profiles of gases*** | WACCM v6 40 years average |
| | $H_2O$: Daily average of the pre-retrieval from following 4 micro windows (MWs): |
| | 2611.4 – 2613.4 $cm^{-1}$, |
| | 2659.0 – 2661.0 $cm^{-1}$, |
| | 2819.0 – 2819.8 $cm^{-1}$, |
| | 2929.8 – 2931.4 $cm^{-1}$. |

*When different settings are used, they are mentioned in individual retrieval.

As for the measurement setting 6M (MCT detector), we changed the aperture size twice. At the start of the measurements with an MCT detector in 2014, we selected the aperture size of 0.8 mm to avoid the zero-level offset due to nonlinearity of the MCT detector. The observed spectra have almost no offset, but S/N was not enough for recoding small absorption feature. Then, the aperture size was changed to 1.15 mm from January 10, 2017. The S/N of the spectra became better and there was still almost no offset. But we found that more S/N were needed to retrieve the species with small absorptions like halocarbons. Finally, the aperture size was changed to 1.7 mm from June 7, 2018. In this case there is some offset and zero-level correction is needed in the analysis but S/N become much better. The sample spectra for the 3 aperture settings were shown in Figure 1.

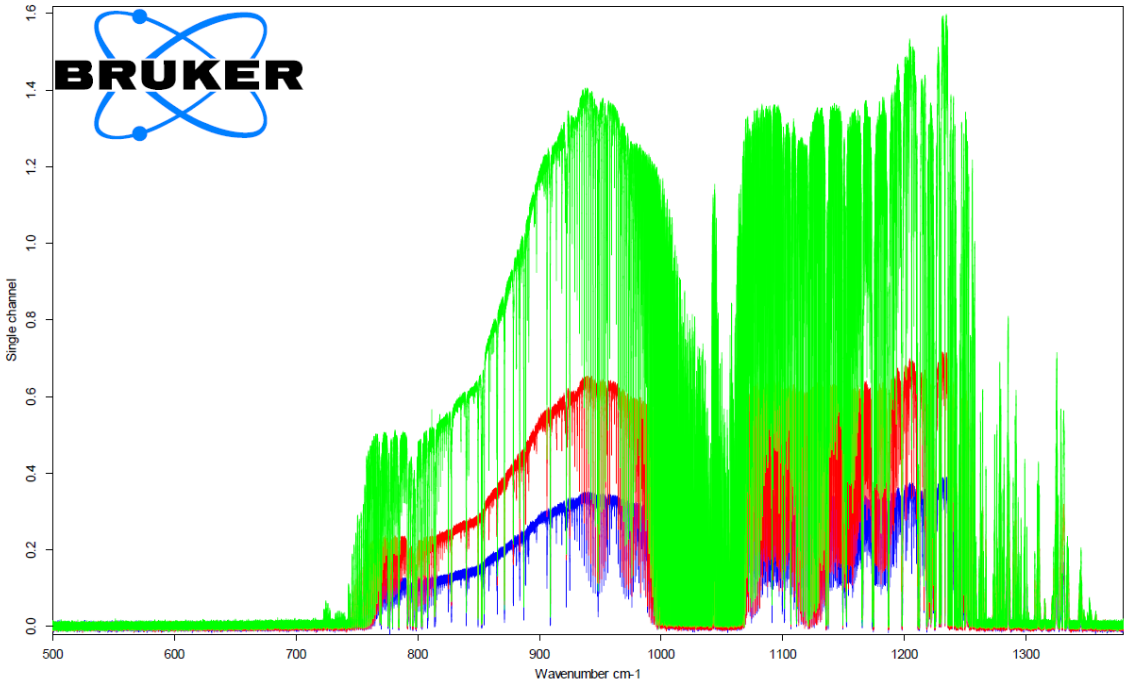


Figure 1. Sample spectra for the 3 aperture settings observed on January 31, 2014 (aperture = 0.8 mm: blue), January 25, 2017 (aperture = 1.15 mm: red), and January 30, 2019 (aperture = 1.7 mm: green).

The retrieved species are as follows:

Default 10 species: $O_3$, $HNO_3$, HCl, HF, CO, $N_2O$, $CH_4$, HCN, $C_2H_6$, $ClONO_2$,

Others: HCHO, OCS, $NH_3$, $C_2H_2$, $NO_2$.

## 4.1 $O_3$

The observed parameters for the sample spectrum shown in Figure 2 are as follows.

| | |
|---|---|
| Timestamp | 2021-01-19 09:26:30 LT |
| SZA (degree) | 65.82 |
| Wavenumber range ($cm^{-1}$) | 500 – 1380 |
| OPD (cm) | 257 |
| Resolution ($cm^{-1}$) | 0.0035 |
| Recording duration (s) | 411 |

The retrieval for $O_3$ was performed using Vigouroux et al. [2008] and Vigouroux et al. [2015] as references. The retrieval parameters for $O_3$ and the results for the sample spectrum shown in Figure 2 are as follows.

| | |
|---|---|
| Microwindow ($cm^{-1}$) | 1000.0 – 1005.0 |
| Interfering molecules | $H_2O$, $C_2H_4$, $CO_2$, $^{668}O_3$, $^{686}O_3$ |
| A priori profiles | WACCM v6 40 years average |
| | $H_2O$: pre-retrieval from 824.4 - 825.9 $cm^{-1}$ |

| | |
|---|---|
| A priori covariance matrix | 30%/SQRT(km) diagonal<br>15 km HWHM Exponential off-diagonal |
| OPD (cm) | 132 |
| Root mean square of residuals (RMS) | 0.544 % |
| Retrieved VCA | 8.280 x $10^{18}$ molecules/$cm^2$ (308.2 DU) |
| Degree of Freedoms (DOFS) | 5.508 |

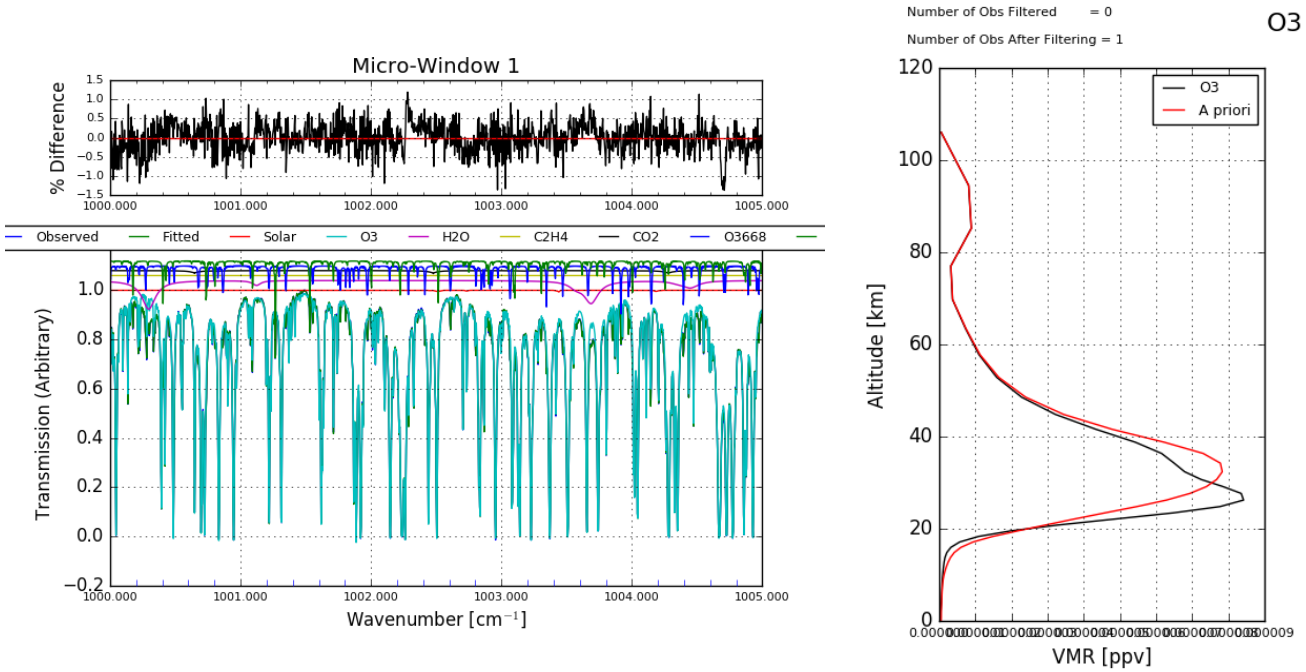


Figure 2. $O_3$ retrieval results for the spectrum observed at 09:26:30 LT on Jan. 19, 2021.

Zero-level correction:

There are some saturated lines in the microwindow for $O_3$ retrieval. Therefore, we use optimized 2nd polynomial fit to fully absorbed regions in 10 μm region calculated in <pspec> and also perform baselincorrect in <sfit4> for all spectra.

Validation for $O_3$ columns

Brewer and ozonesonde observations at Tateno were used to validate the retrieved total column and profile for the observation on same days in 2019. Tsukuba site has an advantage, in that the Tateno (JMA's aerological observatory) is located close to our site. The left panel of Figure 3 shows the FTIR/Brewer ratios observed in 2019. The total columns by FTIR show 4.9 % higher in average than Brewer and the standard deviation is 2.4 %, which agree with Vigouroux, et al. [2008]. This 5 % of bias may be due to the uncertainty of the line intensity.

After the height resolution matching using averaging kernels, the profiles from FTIR and ozonesonde agree within 10% between 18 and 35 km. Comparison for the 15-day (58 spectra) observations (right panel of Figure 3) shows the FTIR/sonde partial column ratio of 1.02 ± 0.05, 1.11

± 0.19, and 1.03 ± 0.05 for 0 - 9.8 km, 9.8 - 18.3 km, and 18.3 - 27.7 km, respectively, indicating good agreement within ~10%.

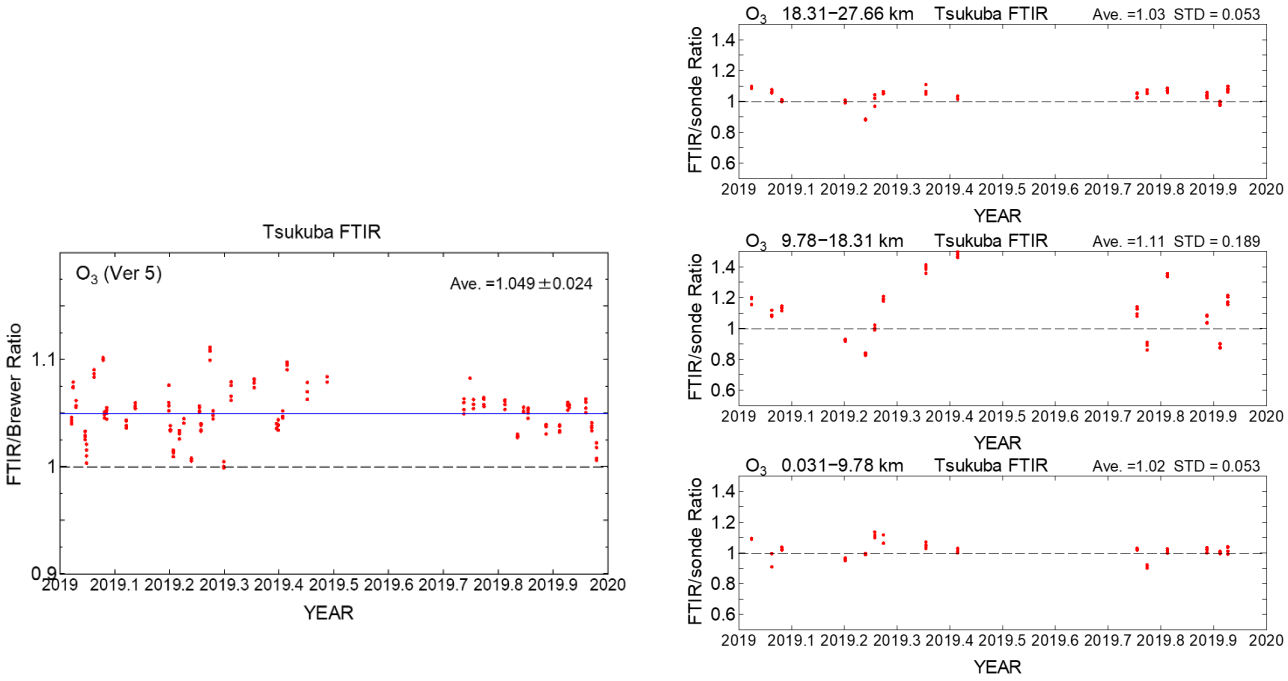


Figure 3. Validation results for $O_3$ total column (left) and partial columns (right).

4.2 $HNO_3$

The observed parameters for the sample spectrum shown in Figure 4 are as follows.

| | |
|---|---|
| Timestamp | 2021-01-25 09:24:14 LT |
| SZA (degree) | 65.14 |
| Wavenumber range ($cm^{-1}$) | 500 – 1380 |
| OPD (cm) | 257 |
| Resolution ($cm^{-1}$) | 0.0035 |
| Recording duration (s) | 411 |

The retrieval parameters for $HNO_3$ and the results for the sample spectrum shown in Figure 4 are as follows.

| | |
|---|---|
| Microwindow ($cm^{-1}$) | 867.05 – 870.0 |
| Interfering molecules | $H_2O$, OCS, $CO_2$, $NH_3$ |
| A priori profiles | WACCM v6 40 years average |
| | $H_2O$: Daily average of the pre-retrieval from 4MWs |
| A priori covariance matrix | 30%/SQRT(km) diagonal |
| | 3 km HWHM Exponential off-diagonal |
| OPD (cm) | 132 |
| Root mean square of residuals (RMS) | 0.279 % |

| | |
|---|---|
| Retrieved VCA | 1.489 x $10^{16}$ molecules/$cm^2$ |
| Degree of Freedoms (DOFS) | 2.401 |

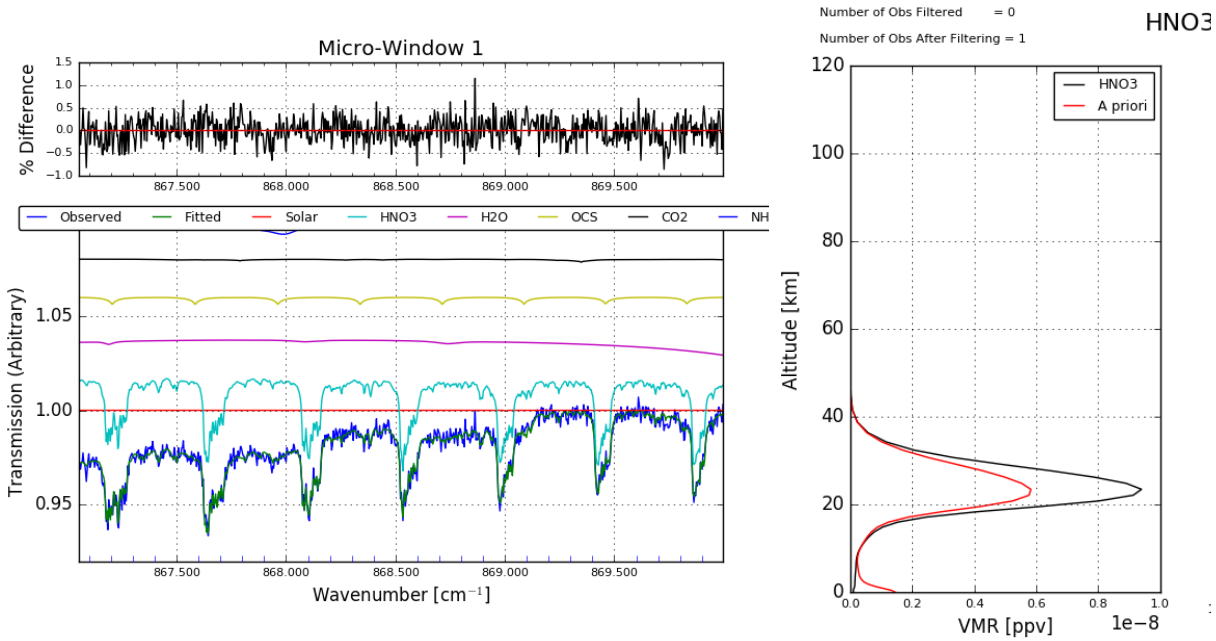


Figure 4. $HNO_3$ retrieval results for the spectrum observed at 09:24:14 LT on Jan. 25, 2021.

Zero-level correction:

There is no saturated line in the microwindow for $HNO_3$ retrieval. Therefore, we use optimized 2nd polynomial fit to fully absorbed regions in 10 μm region calculated in <pspec> and no correction in <sfit4> for the spectra observed with the aperture size of 1.7 mm (after June 7, 2018). For the spectra observed with the aperture size of 0.8 mm or 1.15 mm (before June 1, 2018), no zero-level correction is performed.

4.3 HCl

The observed parameters for the sample spectrum shown in Figure 5 are as follows.

| | |
|---|---|
| Timestamp | 2021-01-13 10:54:43 LT |
| SZA (degree) | 58.88 |
| Wavenumber range ($cm^{-1}$) | 2400 – 3200 |
| OPD (cm) | 257 |
| Resolution ($cm^{-1}$) | 0.0035 |
| Recording duration (s) | 410 |

The retrieval parameters for HCl and the results for the sample spectrum shown in Figure 5 are as follows.

| | |
|---|---|
| Microwindows ($cm^{-1}$) | 2727.73 – 2727.83 |
| | 2775.70 – 2775.80 |
| | 2925.80 – 2926.00 |
| Interfering molecules | $N_2O$, $NO_2$, $CH_4$, HDO, $O_3$ |
| A priori profiles | WACCM v6 40 years average |
| | $H_2O$: Daily average of the pre-retrieval from 4MWs |
| A priori covariance matrix | 30%/SQRT(km) diagonal |
| | 4 km HWHM Exponential off-diagonal |
| OPD (cm) | 257 |
| Root mean square of residuals (RMS) | 0.103 % |
| Retrieved VCA | 3.182 x $10^{15}$ molecules/$cm^2$ |
| Degree of Freedoms (DOFS) | 2.616 |

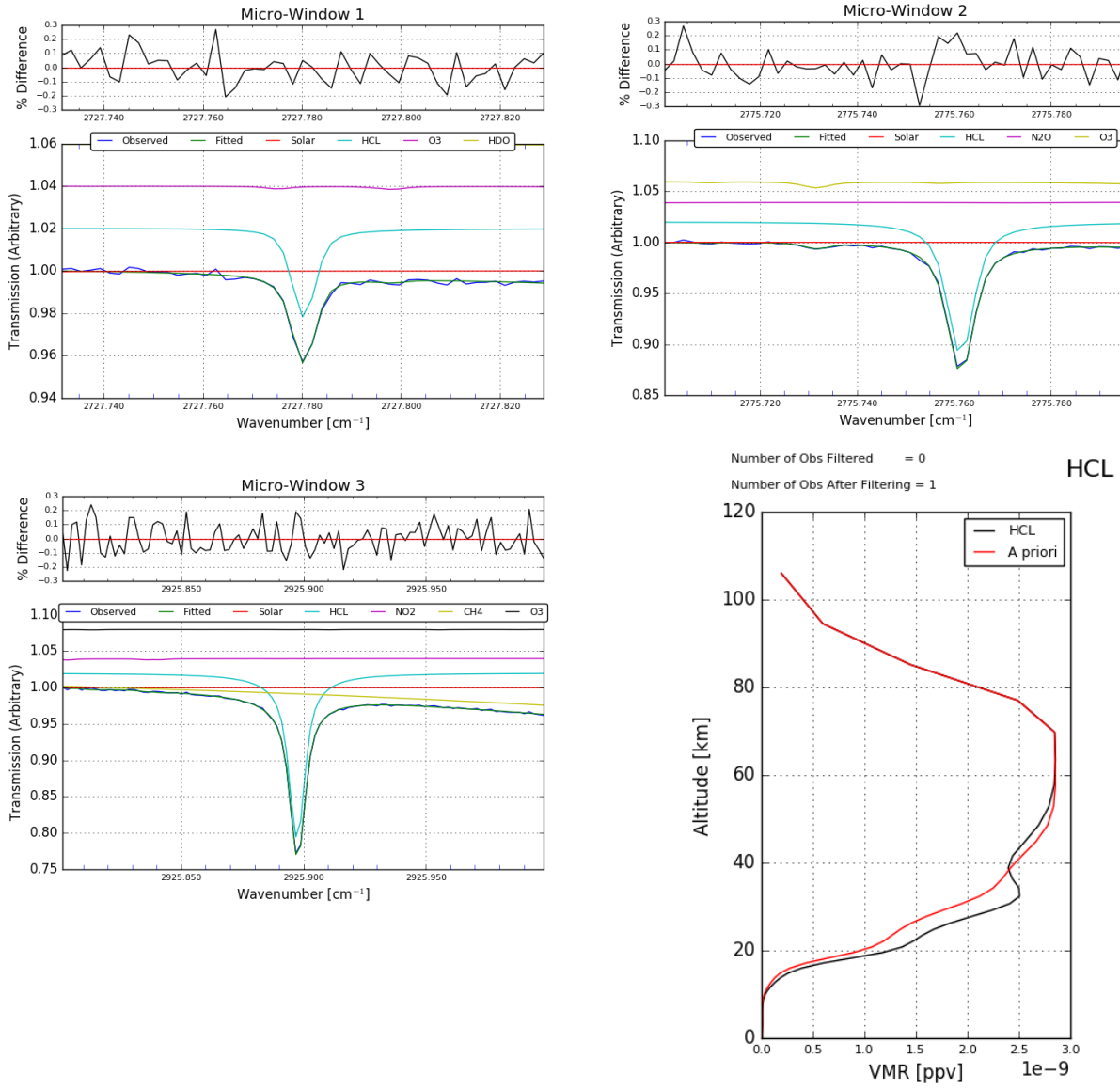


Figure 5. HCl retrieval results for the spectrum observed at 10:54:43 LT on Jan. 13, 2021.

4.4 HF

The observed parameters for the sample spectrum shown in Figure 6 are as follows.

| | |
|---|---|
| Timestamp | 2021-01-13 10:39:58 LT |
| SZA (degree) | 59.73 |
| Wavenumber range ($cm^{-1}$) | 3900 – 4400 |
| OPD (cm) | 257 |
| Resolution ($cm^{-1}$) | 0.0035 |
| Recording duration (s) | 411 |

The retrieval parameters for HF and the results for the sample spectrum shown in Figure 6 are as follows.

| | |
|---|---|
| Microwindow ($cm^{-1}$) | 4038.81 – 4039.07 |
| Interfering molecules | $H_2O$, $CH_4$, HDO |
| A priori profiles | WACCM v6 40 years average |
| | $H_2O$: Daily average of the pre-retrieval from 4MWs |
| A priori covariance matrix | 30%/SQRT(km) diagonal |
| | 4 km HWHM Exponential off-diagonal |
| OPD (cm) | 257 |
| Root mean square of residuals (RMS) | 0.339 % |
| Retrieved VCA | 1.418 x $10^{15}$ molecules/$cm^2$ |
| Degree of Freedoms (DOFS) | 1.778 |

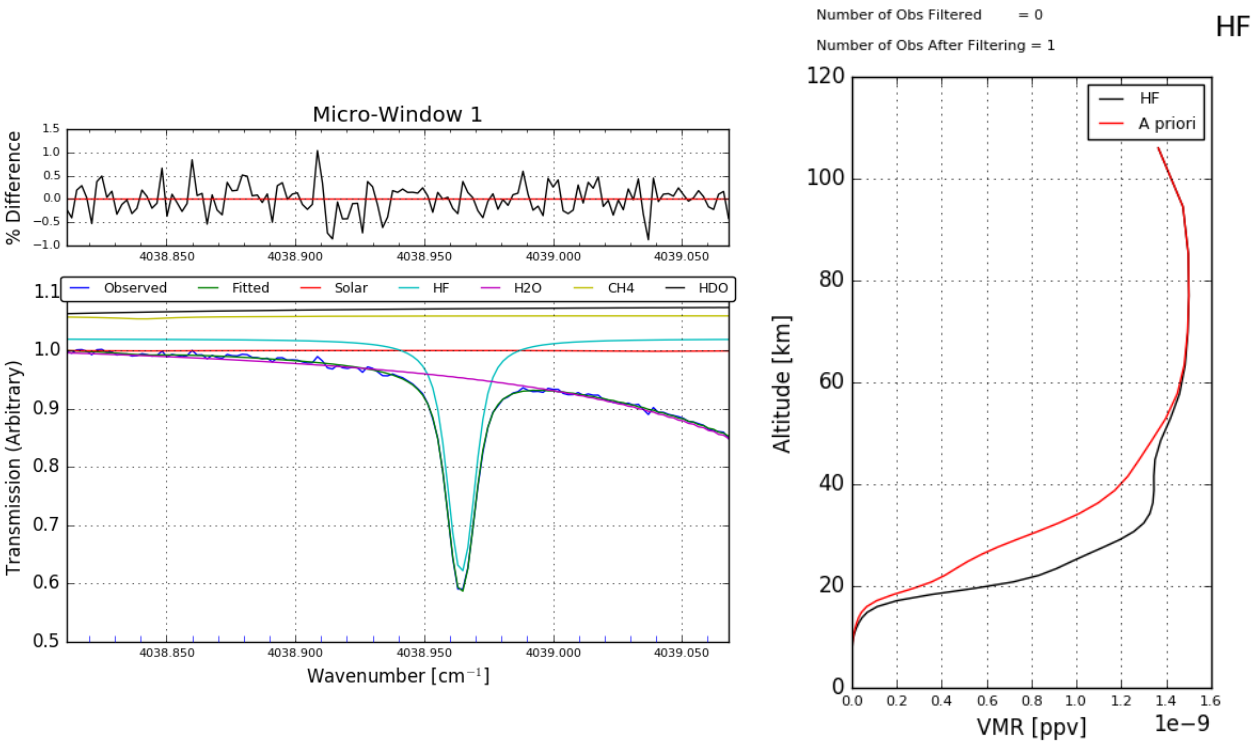


Figure 6. HF retrieval results for the spectrum observed at 10:39:58 LT on Jan. 13, 2021.

4.5 CO

The observed parameters for the sample spectrum shown in Figure 7 are as follows.

| | |
|---|---|
| Timestamp | 2020-12-25 10:51:26 LT |
| SZA (degree) | 60.52 |
| Wavenumber range ($cm^{-1}$) | 1900 – 2800 |
| OPD (cm) | 257 |
| Resolution ($cm^{-1}$) | 0.0035 |
| Recording duration (s) | 411 |

The retrieval parameters for CO and the results for the sample spectrum shown in Figure 7 are as follows.

| | |
|---|---|
| Microwindows ($cm^{-1}$) | 2057.70 – 2058.00 |
| | 2069.56 – 2069.76 |
| | 2157.50 – 2159.15 |
| Interfering molecules | $H_2O$, $N_2O$, OCS, $CO_2$, $O_3$ |
| A priori profiles | WACCM v6 40 years average |
| | $H_2O$: Daily average of the pre-retrieval from 4MWs |
| A priori covariance matrix | 30%/SQRT(km) diagonal |
| | 2 km HWHM Exponential off-diagonal |
| OPD (cm) | 180 |
| Root mean square of residuals (RMS) | 0.477 % |
| Retrieved VCA | 2.474 x $10^{18}$ molecules/$cm^2$ |
| Degree of Freedoms (DOFS) | 3.072 |

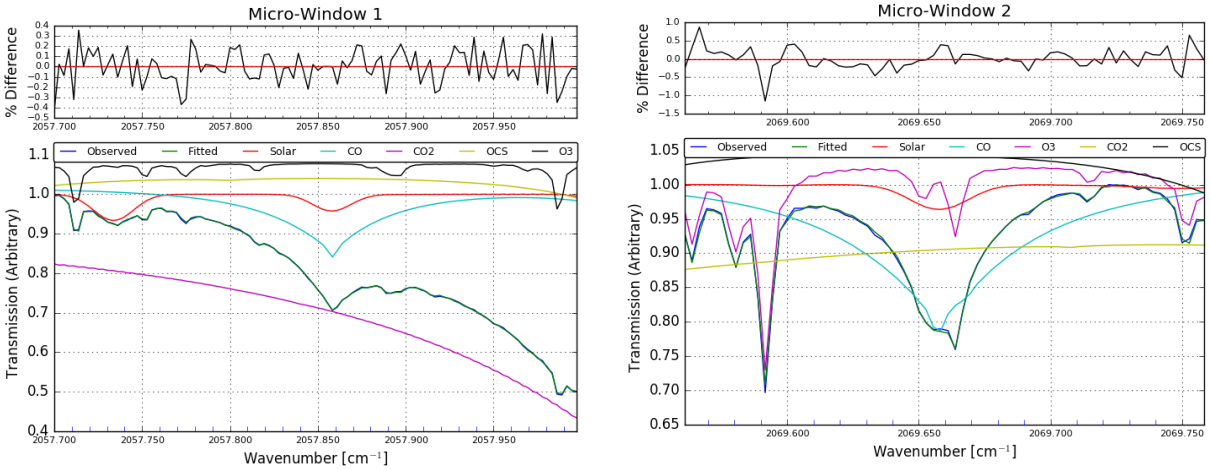

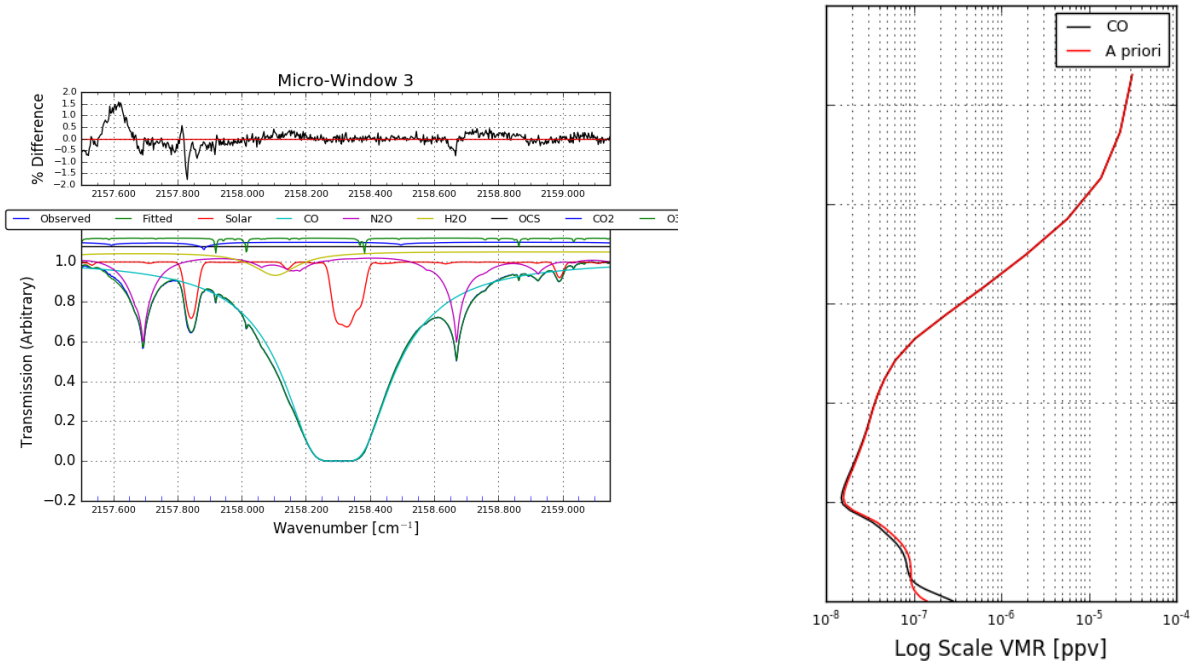


Figure 7. CO retrieval results for the spectrum observed at 10:51:26 LT on Dec. 25, 2020.

4.6 $N_2O$

The observed parameters for the sample spectrum shown in Figure 8 are as follows.

| | |
|---|---|
| Timestamp | 2021-01-21 10:41:35 LT |
| SZA (degree) | 58.28 |
| Wavenumber range ($cm^{-1}$) | 1900 – 2800 |
| OPD (cm) | 257 |
| Resolution ($cm^{-1}$) | 0.0035 |
| Recording duration (s) | 411 |

The retrieval parameters for $N_2O$ and the results for the sample spectrum shown in Figure 8 are as follows.

| | |
|---|---|
| Microwindows ($cm^{-1}$) | 2481.30 – 2482.60 |
| | 2526.40 – 2528.20 |
| | 2537.85 – 2538.80 |
| | 2540.10 – 2540.70 |
| Interfering molecules | $H_2O$, HDO, $CO_2$, $CH_4$ |
| A priori profiles | WACCM v6 40 years average |
| | $H_2O$: Daily average of the pre-retrieval from 4MWs |
| A priori covariance matrix | 30%/SQRT(km) diagonal |
| | 1000 km HWHM Exponential off-diagonal |
| OPD (cm) | 257 |

| | |
|---|---|
| Root mean square of residuals (RMS) | 0.137 % |
| Retrieved VCA | 6.878 x $10^{18}$ molecules/$cm^2$ |
| Degree of Freedoms (DOFS) | 3.731 |

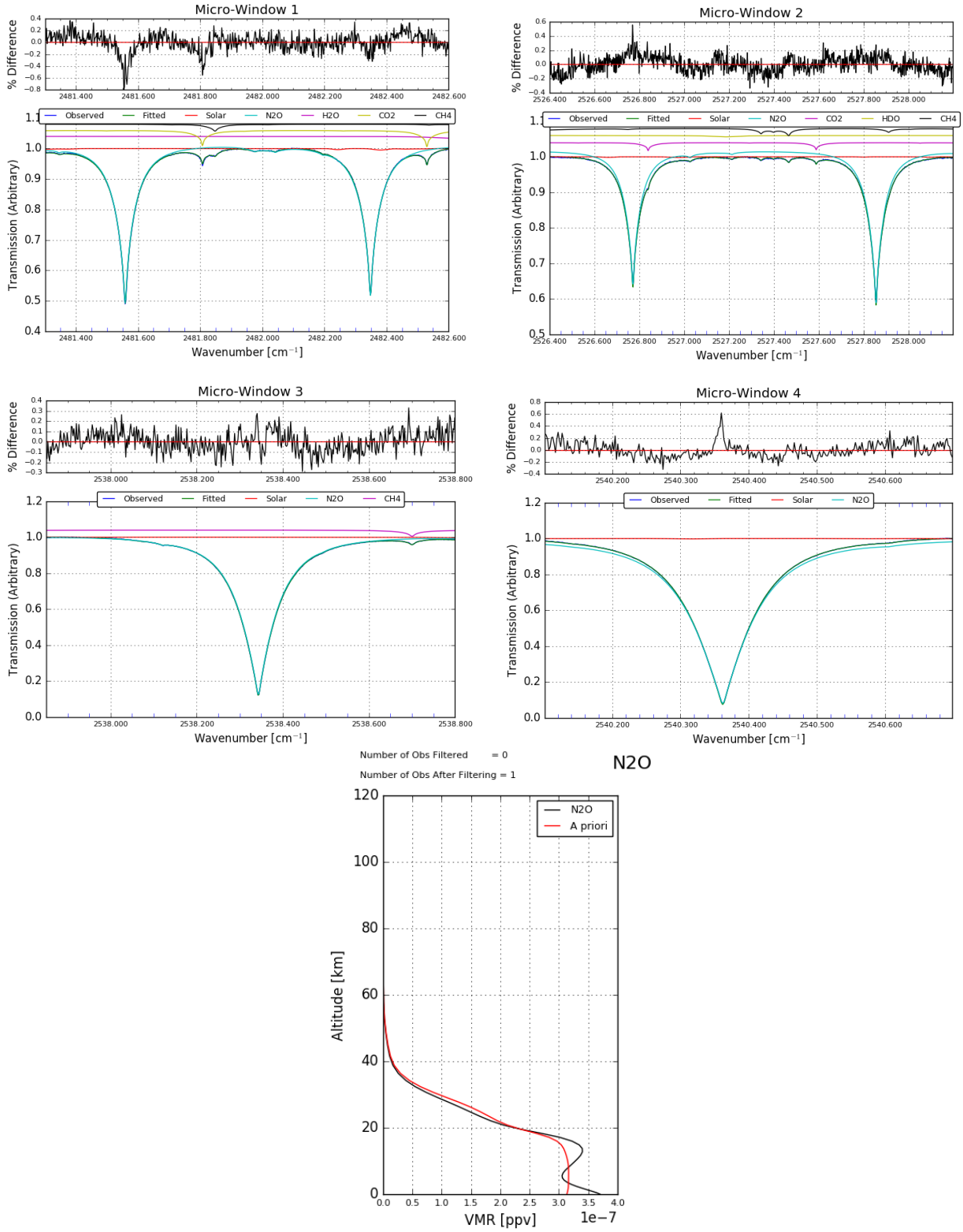


Figure 8. $N_2O$ retrieval results for the spectrum observed at 10:41:35 LT on Jan. 21, 2021.

4.7 $CH_4$

The observed parameters for the sample spectrum shown in Figure 9 are as follows.

| | |
|---|---|
| Timestamp | 2020-12-25 10:44:01 LT |
| SZA (degree) | 60.87 |
| Wavenumber range ($cm^{-1}$) | 2400 – 3200 |
| OPD (cm) | 257 |
| Resolution ($cm^{-1}$) | 0.0035 |
| Recording duration (s) | 410 |

The retrieval for $CH_4$ was performed using Sussmann et al. [2011] as a reference. The retrieval parameters for $CH_4$ and the results for the sample spectrum shown in Figure 9 are as follows.

| | |
|---|---|
| Microwindows ($cm^{-1}$) | 2613.70 – 2615.40 |
| | 2835.50 – 2835.80 |
| | 2921.00 – 2921.60 |
| Interfering molecules | $H_2O$, HDO, $NO_2$, $CO_2$ |
| A priori profiles | WACCM v6 40 years average |
| | $H_2O$: Daily average of the pre-retrieval from 4MWs |
| A priori covariance matrix | 7%/SQRT(km) diagonal |
| | 4 km HWHM Exponential off-diagonal |
| OPD (cm) | 132 |
| Root mean square of residuals (RMS) | 0.129% |
| Retrieved VCA | 4.020 x $10^{19}$ molecules/$cm^2$ |
| Degree of Freedoms (DOFS) | 3.469 |

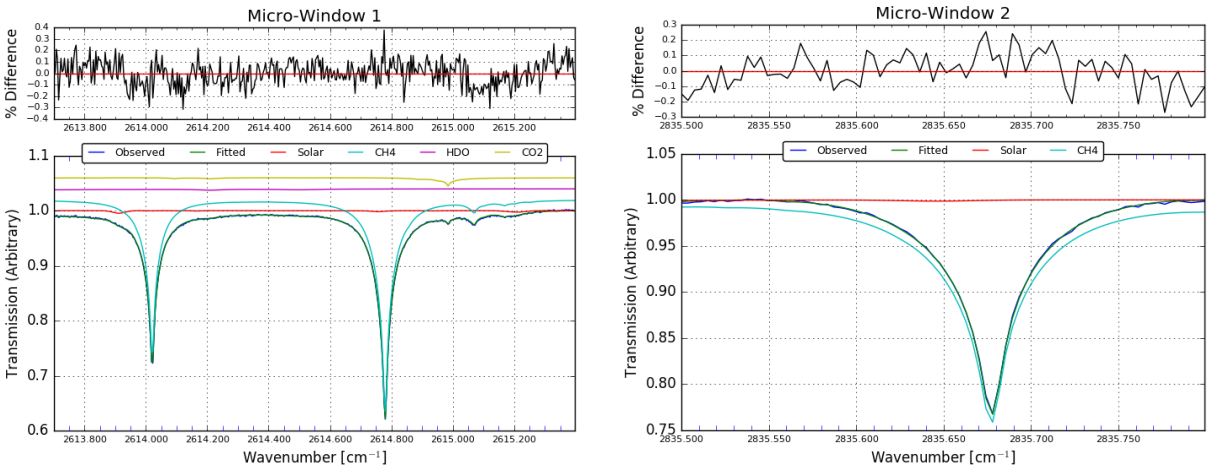

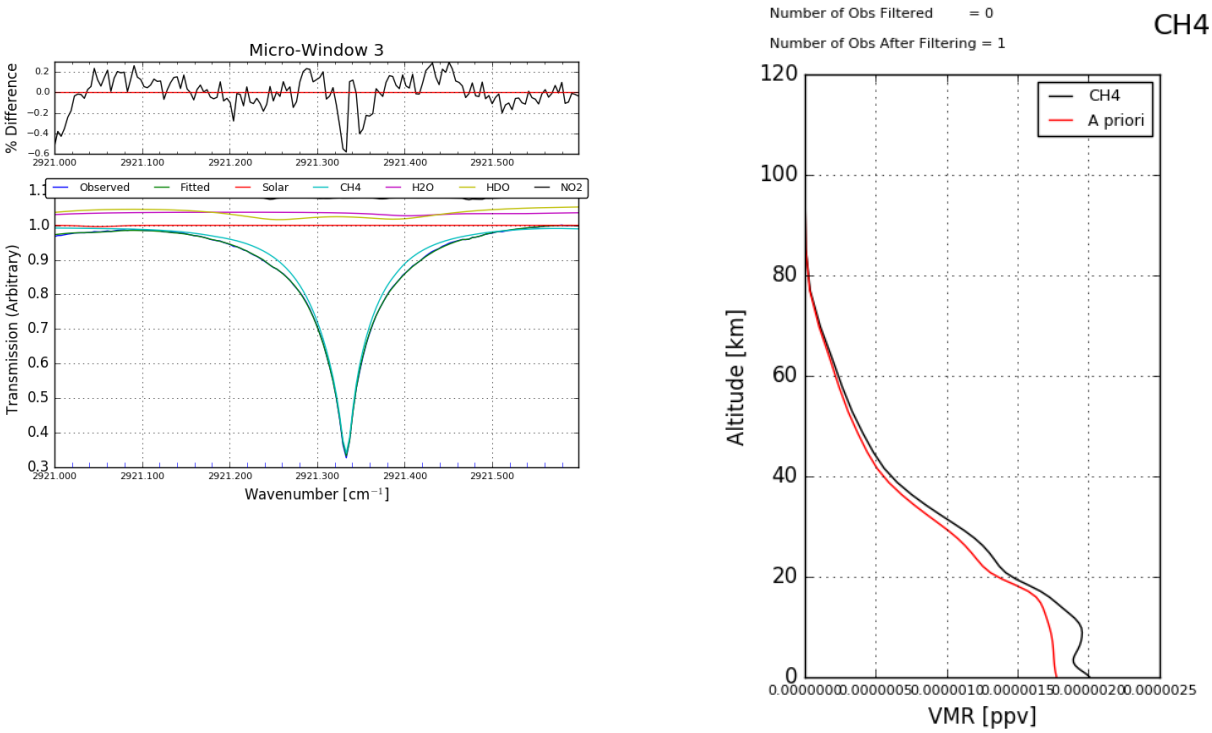


Figure 9. $CH_4$ retrieval results for the spectrum observed at 10:44:01 LT on Dec. 25, 2020.

4.8 HCN

The observed parameters for the sample spectrum shown in Figure 10 are as follows.

| | |
|---|---|
| Timestamp | 2019-01-09 09:03:27 LT |
| SZA (degree) | 69.80 |
| Wavenumber range ($cm^{-1}$) | 2800 – 3700 |
| OPD (cm) | 257 |
| Resolution ($cm^{-1}$) | 0.0035 |
| Recording duration (s) | 410 |

The retrieval parameters for HCN and the results for the sample spectrum shown in Figure 10 are as follows.

| | |
|---|---|
| Microwindows ($cm^{-1}$) | 3268.04 – 3268.40 |
| | 3287.10 – 3287.35 |
| | 3299.40 – 3299.60 |
| Interfering molecules | $H_2O$, $C_2H_2$, $CO_2$, $O_3$ |
| A priori profiles | WACCM v6 40 years average |
| | $H_2O$: Daily average of the pre-retrieval from 4MWs |
| A priori covariance matrix | 30%/SQRT(km) diagonal |
| | 6 km HWHM Exponential off-diagonal |
| OPD (cm) | 180 |
| Root mean square of residuals (RMS) | 0.113% |

| | |
|---|---|
| Retrieved VCA | 4.083 x $10^{15}$ molecules/$cm^2$ |
| Degree of Freedoms (DOFS) | 3.020 |

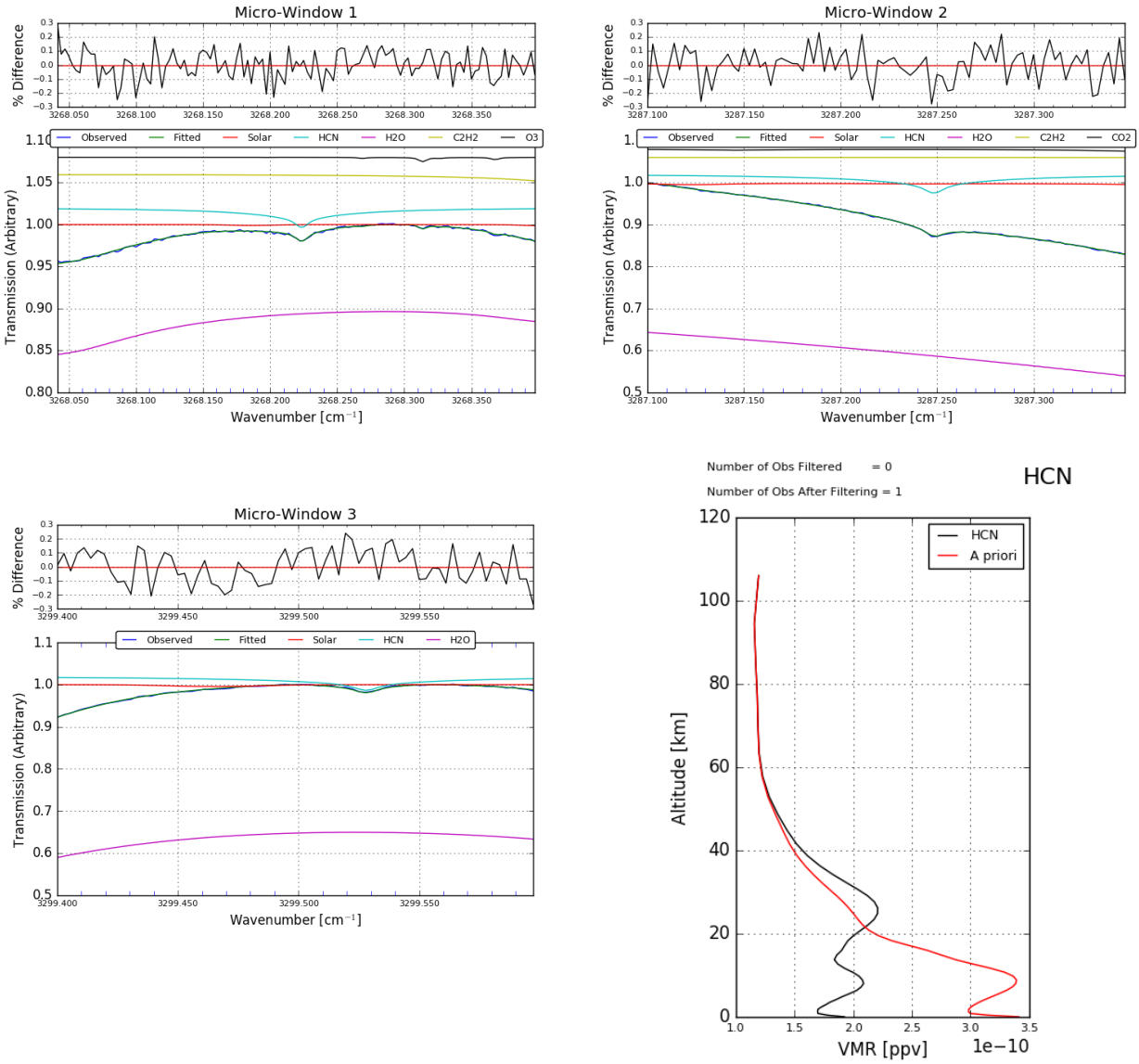


Figure 10. HCN retrieval results for the spectrum observed at 09:03:27 LT on Jan. 09, 2019.

## 4.9 $C_2H_6$

The observed parameters for the sample spectrum shown in Figure 11 are as follows.

| | |
|---|---|
| Timestamp | 2020-12-25 10:44:01 LT |
| SZA (degree) | 60.87 |
| Wavenumber range ($cm^{-1}$) | 2400 – 3200 |
| OPD (cm) | 257 |
| Resolution ($cm^{-1}$) | 0.0035 |
| Recording duration (s) | 410 |

The retrieval for $C_2H_6$ was performed using Franco et al. [2015] as a reference. The retrieval parameters for $C_2H_6$ and the results for the sample spectrum shown in Figure 11 are as follows.

| | |
|---|---|
| Microwindows ($cm^{-1}$) | 2976.660 – 2977.059 |
| | 2983.200 – 2983.500 |
| Interfering molecules | $H_2O$, $O_3$, $CH_4$, $CH_3Cl$ |
| Spectroscopy | Pseudolines produced by G. C. Toon |
| A priori profiles | WACCM v6 40 years average |
| | $C_2H_6$: 2.8 x WACCM v6 40 years average |
| | $H_2O$: Daily average of the pre-retrieval from 4MWs |
| A priori covariance matrix | CHASER statistics diagonal |
| | 4 km HWHM Exponential off-diagonal |
| OPD (cm) | 180 |
| Root mean square of residuals (RMS) | 0.128% |
| Retrieved VCA | 2.359 x $10^{16}$ molecules/$cm^2$ |
| Degree of Freedoms (DOFS) | 2.108 |

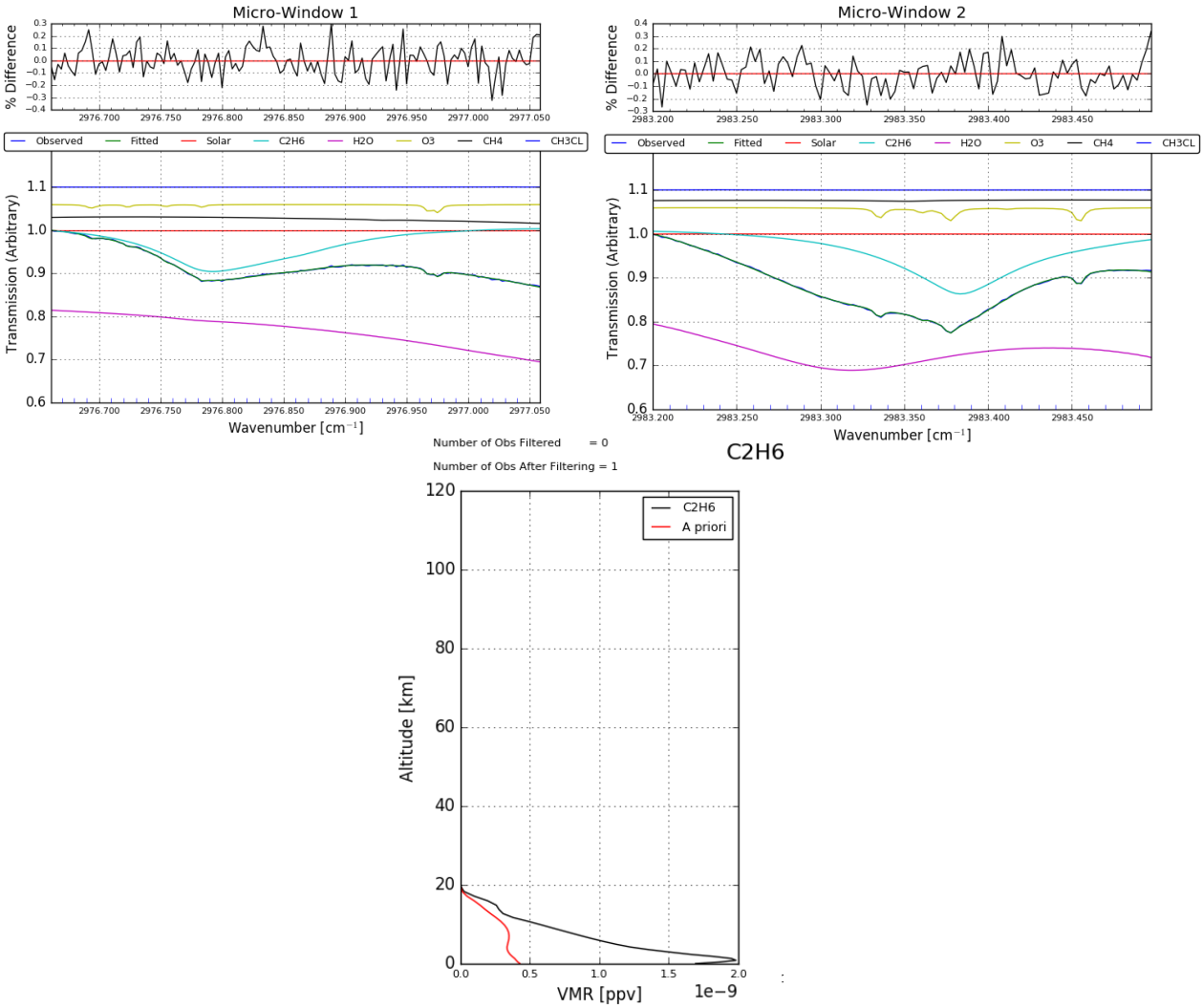


Figure 11. $C_2H_6$ retrieval results for the spectrum observed at 10:44:01 LT on Dec. 25, 2020.

4.10 $ClONO_2$

The observed parameters for the sample spectrum shown in Figure 12 are as follows.

| | |
|---|---|
| Timestamp | 2021-01-25 09:24:14 LT |
| SZA (degree) | 65.14 |
| Wavenumber range ($cm^{-1}$) | 500 – 1380 |
| OPD (cm) | 257 |
| Resolution ($cm^{-1}$) | 0.0035 |
| Recording duration (s) | 411 |

The retrieval for $ClONO_2$ was performed using parameters for Jungfraujoch (E. Mahieu, private communication) as a reference. The retrieval parameters for $ClONO_2$ and the results for the sample spectrum shown in Figure 12 are as follows.

| | |
|---|---|
| Microwindow ($cm^{-1}$) | 779.30 – 780.60 |
| Interfering molecules | O3, $H_2O$, $CO_2$, $HNO_3$, $COF_2$ |
| Spectroscopy | Pseudolines produced by G. C. Toon |
| A priori profiles | WACCM v6 40 years average |
| | $H_2O$: Daily average of the pre-retrieval from 4MWs |
| A priori covariance matrix | 100%/SQRT(km) diagonal |
| | none off-diagonal |
| OPD (cm) | 125 |
| Root mean square of residuals (RMS) | 0.640 % |
| Retrieved VCA | 6.310 x $10^{14}$ molecules/$cm^2$ |
| Degree of Freedoms (DOFS) | 0.859 |

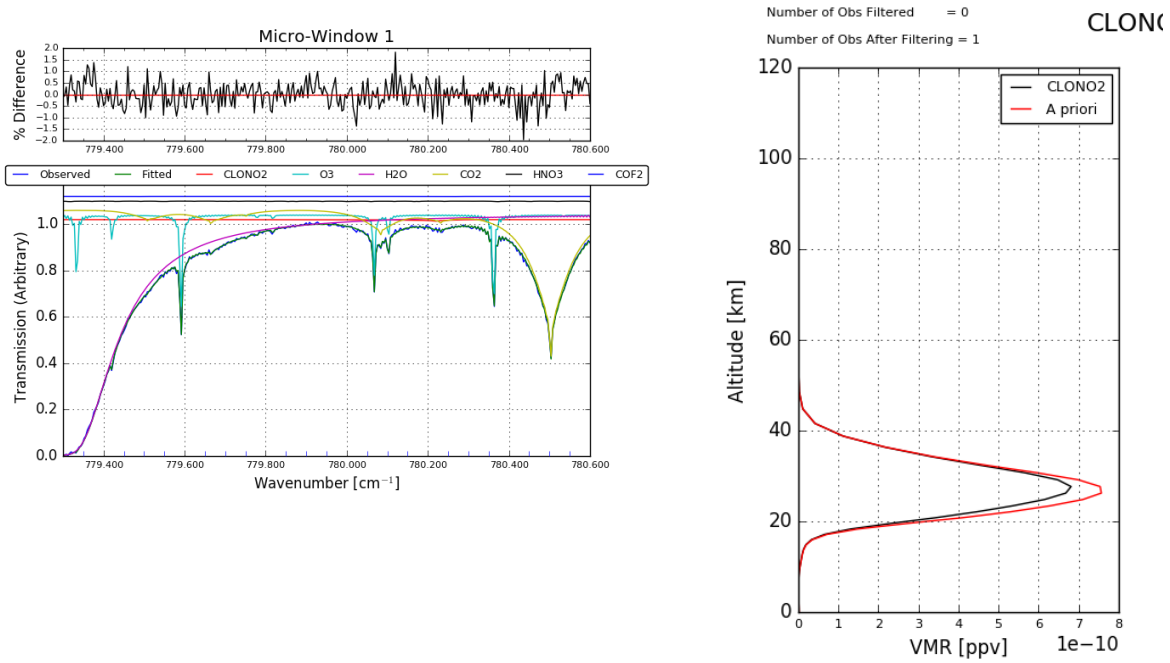


Figure 12. $ClONO_2$ retrieval results for the spectrum observed at 09:24:14 LT on Jan. 25, 2021.

Zero-level correction:

Same as that for $HNO_3$.

4.11 HCHO

The observed parameters for the sample spectrum shown in Figure 13 are as follows.

| | |
|---|---|
| Timestamp | 2020-12-25 10:44:01 LT |
| SZA (degree) | 60.87 |
| Wavenumber range ($cm^{-1}$) | 2400 – 3200 |
| OPD (cm) | 257 |
| Resolution ($cm^{-1}$) | 0.0035 |
| Recording duration (s) | 410 |

The retrieval for HCHO was performed using Vigouroux et al. [2018] as a reference. The retrieval parameters for HCHO and the results for the sample spectrum shown in Figure 13 are as follows.

| | |
|---|---|
| Microwindows ($cm^{-1}$) | 2763.42 – 2764.17 |
| | 2765.65 – 2766.01 |
| | 2778.15 – 2779.10 |
| | 2780.65 – 2782.00 |
| Interfering molecules | $CH_4$, HDO, $N_2O$, $O_3$, $H_2O$ |
| A priori profiles | WACCM v6 40 years average |
| | $H_2O$: Daily average of the pre-retrieval from 4MWs |
| | HDO: copy of $H_2O$ |
| A priori covariance matrix | Tikhonov L1 regularization |
| OPD (cm) | 180 |
| Root mean square of residuals (RMS) | 0.157 % |
| Retrieved VCA | $5.431 \times 10^{15}$ molecules/$cm^2$ |
| Degree of Freedoms (DOFS) | 1.305 |

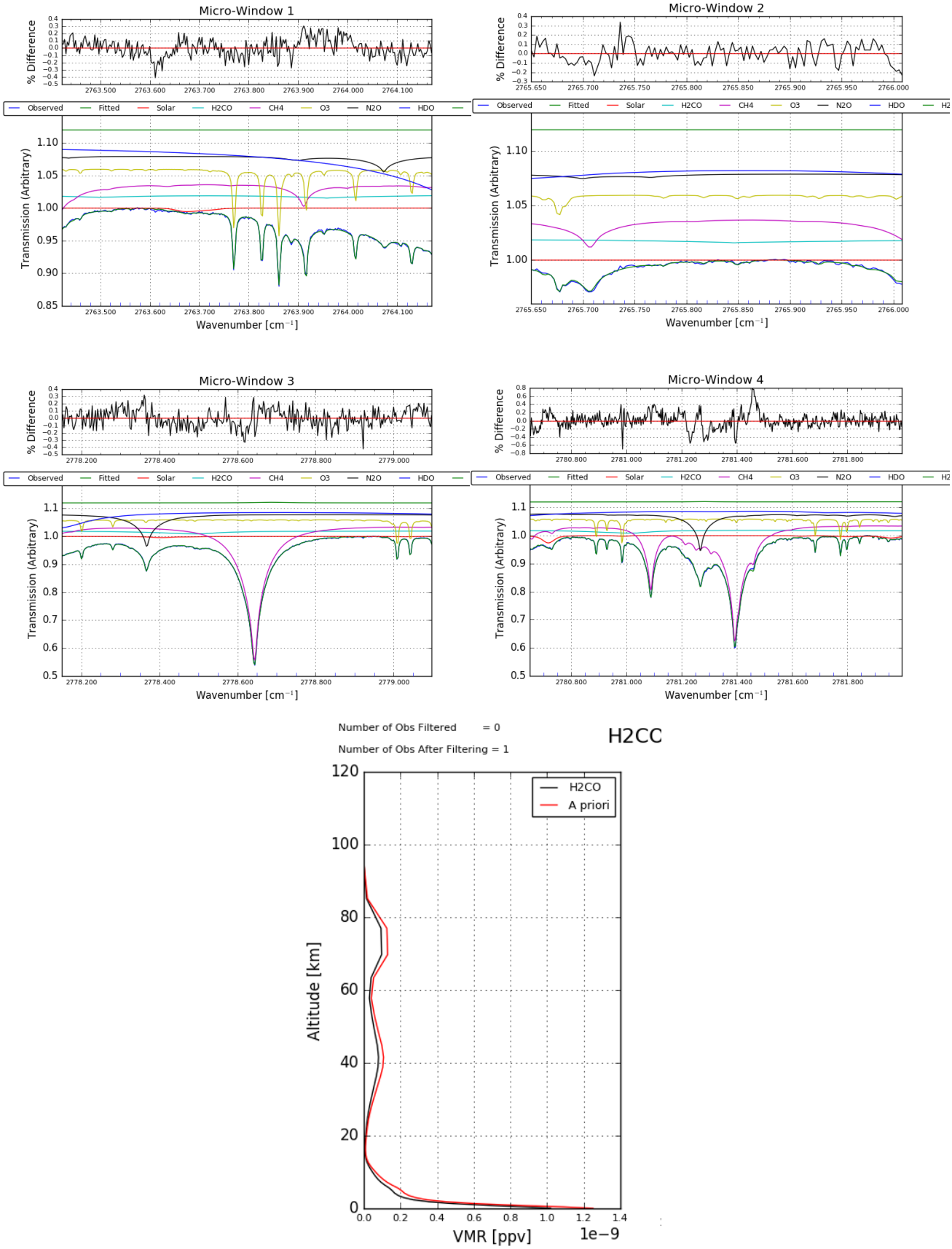


Figure 13. HCHO retrieval results for the spectrum observed at 10:44:01 LT on Dec. 25, 2020.

4.12 OCS

The observed parameters for the sample spectrum shown in Figure 14 are as follows.

| | |
|---|---|
| Timestamp | 2019-01-09 10:55:01 LT |
| SZA (degree) | 59.46 |
| Wavenumber range ($cm^{-1}$) | 1700 – 2200 |
| OPD (cm) | 257 |
| Resolution ($cm^{-1}$) | 0.0035 |
| Recording duration (s) | 411 |

The retrieval for OCS was described in Hannigan et al. [2022] in detail. The retrieval parameters for OCS and the results for the sample spectrum shown in Figure 14 are as follows.

| | |
|---|---|
| Microwindows ($cm^{-1}$) | 2030.75 – 2031.06 |
| | 2047.85 – 2048.24 |
| | 2049.77 – 2050.18 |
| | 2051.18 – 2051.46 |
| | 2054.33 – 2054.67 |
| Interfering molecules | $O_3$, CO, $H_2O$, $H_2{}^{18}O$, $CO^{18}O$, $CO_2$ |
| Spectroscopy | HITRAN2012 |
| A priori profiles | WACCM v6 40 years average |
| | OCS: estimated from HIPPO + ACE-FTS |
| | $H_2O$: Daily average of the pre-retrieval from 4MWs |
| A priori covariance matrix | (1 standard deviation of HIPPO + ACE-FTS) /SQRT(km) diagonal |
| | 4 km HWHM Exponential off-diagonal |
| OPD (cm) | 180 |
| Root mean square of residuals (RMS) | 0.177 % |
| Retrieved VCA | $9.568 \times 10^{15}$ molecules/$cm^2$ |
| Degree of Freedoms (DOFS) | 3.249 |

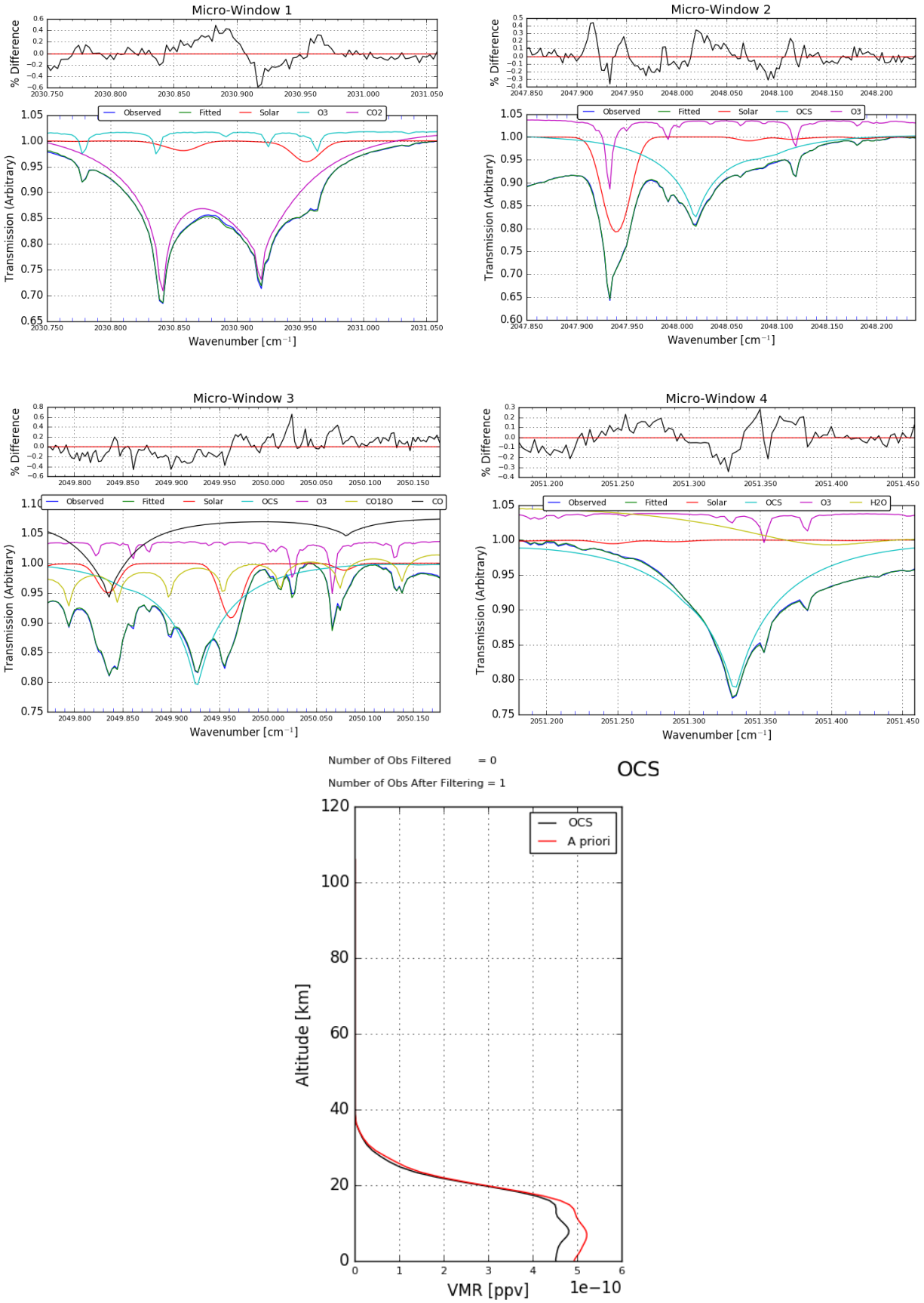


Figure 14. OCS retrieval results for the spectrum observed at 10:55:01 LT on Jan. 09, 2019.

4.13 $NH_3$

The observed parameters for the sample spectrum shown in Figure 15 are as follows.

| | |
|---|---|
| Timestamp | 2020-12-22 09:51:47 LT |
| SZA (degree) | 64.57 |
| Wavenumber range ($cm^{-1}$) | 500 – 1380 |
| OPD (cm) | 129 |
| Resolution ($cm^{-1}$) | 0.0070 |
| Recording duration (s) | 416 |

The retrieval for $NH_3$ was performed using the parameters updated from Dammers et al. [2015]. The retrieval parameters for $NH_3$ and the results for the sample spectrum shown in Figure 15 are as follows.

| | |
|---|---|
| Microwindows ($cm^{-1}$) | 930.320 – 931.320 |
| | 966.970 – 967.675 |
| Interfering molecules | $H_2O$, $O_3$, $CO_2$, $^{13}CO_2$, $CO^{18}O$, $N_2O$, $HNO_3$ |
| A priori profiles | WACCM v6 40 years average |
| | $NH_3$: GEOS-Chem (median) |
| | $H_2O$: Daily average of the pre-retrieval from 4MWs |
| A priori covariance matrix | 100%/SQRT(km) diagonal |
| | 2 km HWHM Exponential off-diagonal |
| OPD (cm) | 132 |
| Root mean square of residuals (RMS) | 0.123 % |
| Retrieved VCA | 4.684 x $10^{15}$ molecules/$cm^2$ |
| Degree of Freedoms (DOFS) | 1.286 |

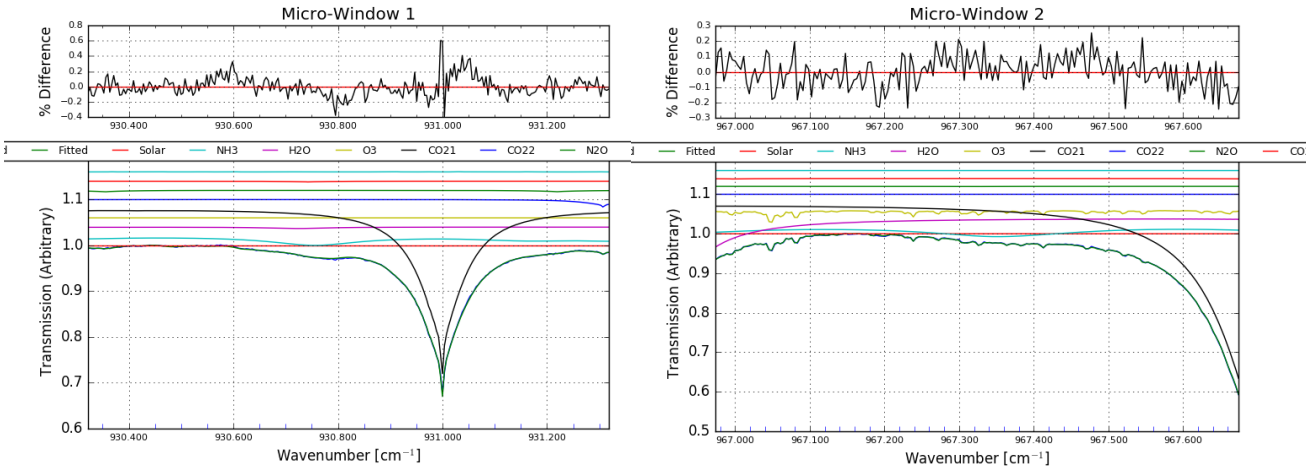

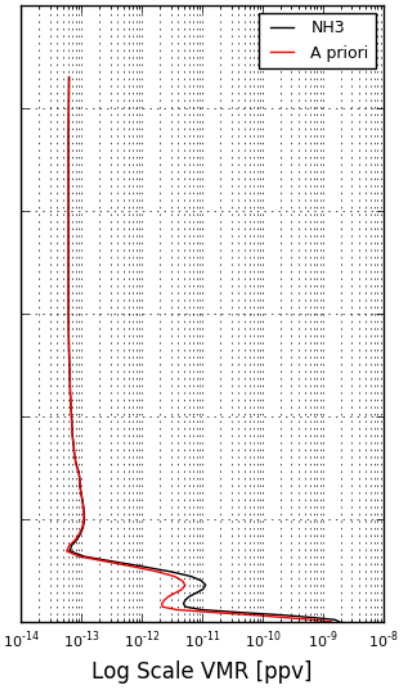


Figure 15. $NH_3$ retrieval results for the spectrum observed at 09:51:47 LT on Dec. 22, 2020.

Zero-level correction:

Same as that for $HNO_3$.

4.14 $C_2H_2$

The observed parameters for the sample spectrum shown in Figure 16 are as follows.

| | |
|---|---|
| Timestamp | 2019-01-09 09:03:27 LT |
| SZA (degree) | 69.80 |
| Wavenumber range ($cm^{-1}$) | 2800 – 3700 |
| OPD (cm) | 257 |
| Resolution ($cm^{-1}$) | 0.0035 |
| Recording duration (s) | 410 |

The retrieval parameters for $C_2H_2$ and the results for the sample spectrum shown in Figure 16 are as follows.

| | |
|---|---|
| Microwindow ($cm^{-1}$) | 3250.25 – 3251.11 |
| Interfering molecules | $H_2O$, $H_2{}^{18}O$ |
| A priori profiles | WACCM v6 40 years average |
| | $H_2O$: Daily average of the pre-retrieval from 4MWs |
| | $H_2{}^{18}O$: copy of $H_2O$ |
| A priori covariance matrix | 30%/SQRT(km) diagonal |

| | |
|---|---|
| | 4 km HWHM Exponential off-diagonal |
| OPD (cm) | 250 |
| Root mean square of residuals (RMS) | 0.137% |
| Retrieved VCA | 5.613 x $10^{15}$ molecules/$cm^2$ |
| Degree of Freedoms (DOFS) | 1.562 |

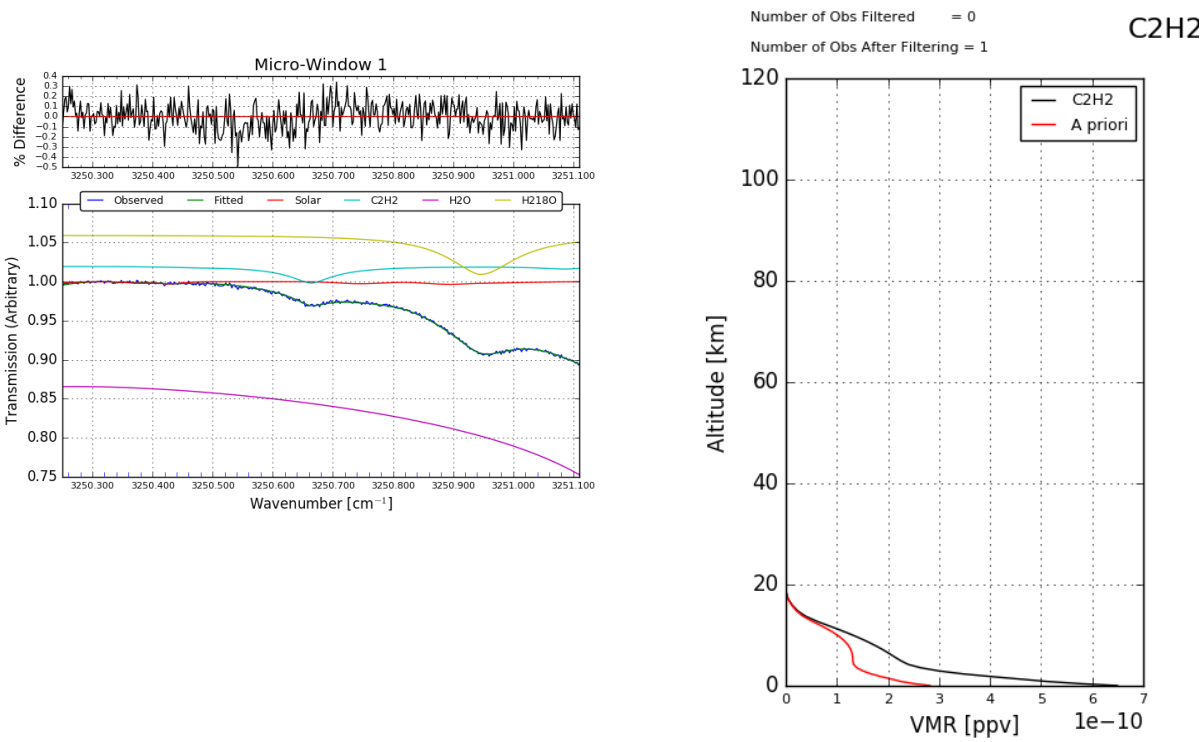


Figure 16. $C_2H_2$ retrieval results for the spectrum observed at 09:03:27 LT on Jan. 09, 2019.

4.15 $NO_2$

The observed parameters for the sample spectrum shown in Figure 17 are as follows.

| | |
|---|---|
| Timestamp | 2020-12-25 10:44:01 LT |
| SZA (degree) | 60.87 |
| Wavenumber range ($cm^{-1}$) | 2400 – 3200 |
| OPD (cm) | 257 |
| Resolution ($cm^{-1}$) | 0.0035 |
| Recording duration (s) | 410 |

The retrieval for $NO_2$ was performed in corporation with C. Vigouroux. The retrieval parameters for $NO_2$ and the results for the sample spectrum shown in Figure 17 are as follows.

| | |
|---|---|
| Microwindow ($cm^{-1}$) | 2914.30 – 2914.85 |
| Interfering molecules | $CH_4$, $H_2O$, $O_3$, $C_2H_6$, HCHO, OCS, $CH_3D$, HDO |
| A priori profiles | WACCM v6 40 years average |
| | $H_2O$: Daily average of the pre-retrieval from 4MWs |

| | |
|---|---|
| | HDO: copy of $H_2O$ |
| A priori covariance matrix | 100%/SQRT(km) diagonal |
| | 4 km HWHM Exponential off-diagonal |
| OPD (cm) | 180 |
| Root mean square of residuals (RMS) | 0.084 % |
| Retrieved VCA | 1.244 x $10^{16}$ molecules/$cm^2$ |
| Degree of Freedoms (DOFS) | 1.875 |

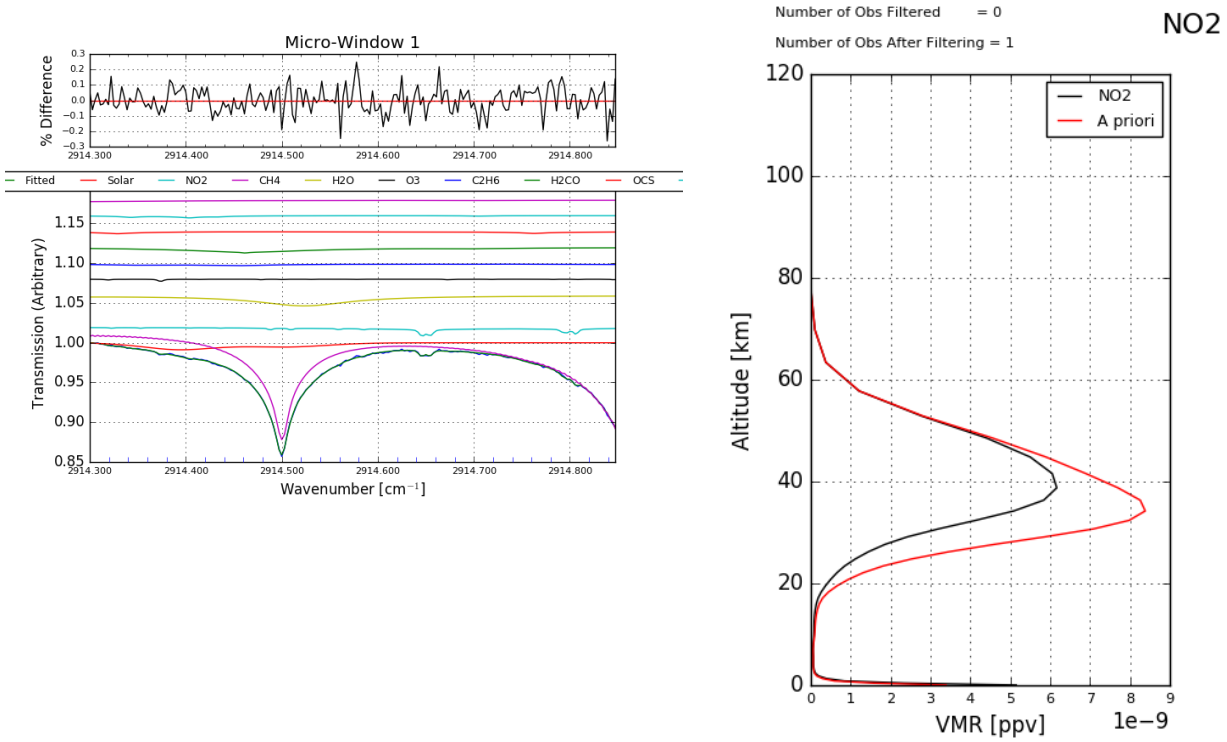


Figure 17. $NO_2$ retrieval results for the spectrum observed at 10:44:01 LT on Dec. 25, 2020.

# 5 HBr cell measurement data

14 spectral lines were used by LINEFIT v.14 in order to deduce the ILS. The 14 microwindows boundaries are displayed in the following table.

| Microwindow number | Microwindow ($cm^{-1}$) |
|---|---|
| 1 | 2412.48 – 2412.88 |
| 2 | 2412.82 – 2413.22 |
| 3 | 2432.18 – 2432.58 |
| 4 | 2432.53 – 2432.93 |
| 5 | 2451.49 – 2451.89 |
| 6 | 2451.84 – 2452.24 |
| 7 | 2470.38 – 2470.78 |
| 8 | 2470.73 – 2471.13 |
| 9 | 2488.84 – 2489.24 |
| 10 | 2489.20 – 2489.60 |
| 11 | 2506.88 – 2507.28 |
| 12 | 2507.25 – 2507.65 |
| 13 | 2524.48 – 2524.88 |
| 14 | 2524.85 – 2525.25 |

*Different microwindows between 2590.32 $cm^{-1}$ and 2675.34 $cm^{-1}$ were used before April 2013.

Figure 18 shows the retrieved modulation efficiency and phase from the HBr spectra taken on May 20, 2013.

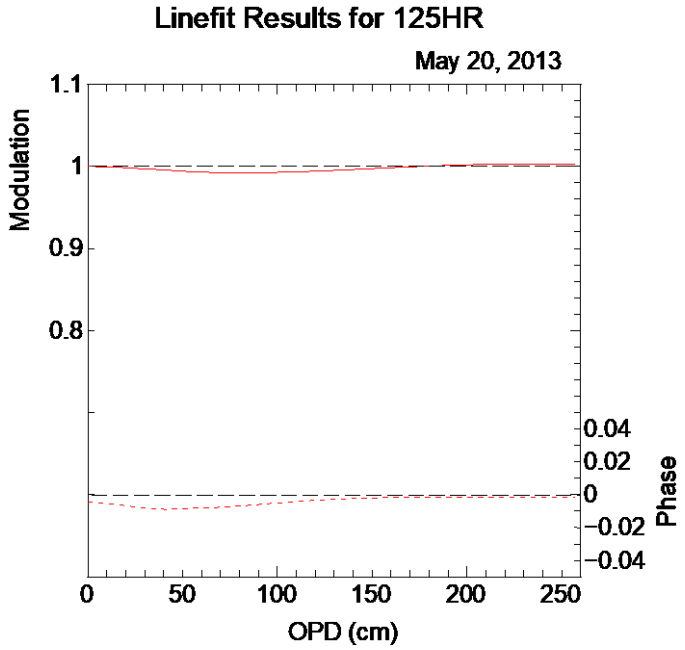


Figure 18. Modulation efficiency and phase retrieved from the HBr spectra taken on May 20, 2013.

As mentioned in Section 2.1, the ILS became worse due to the earthquakes in February 2005 (120HR) and March 2011 (125HR). The modulation efficiencies and phases before and after the earthquakes are shown in Figure 19 (for 120HR) and 20 (for 125HR). Temporal variation of the modulation efficiencies between 2010 and 2012 for 125HR is also shown in Figure 21.

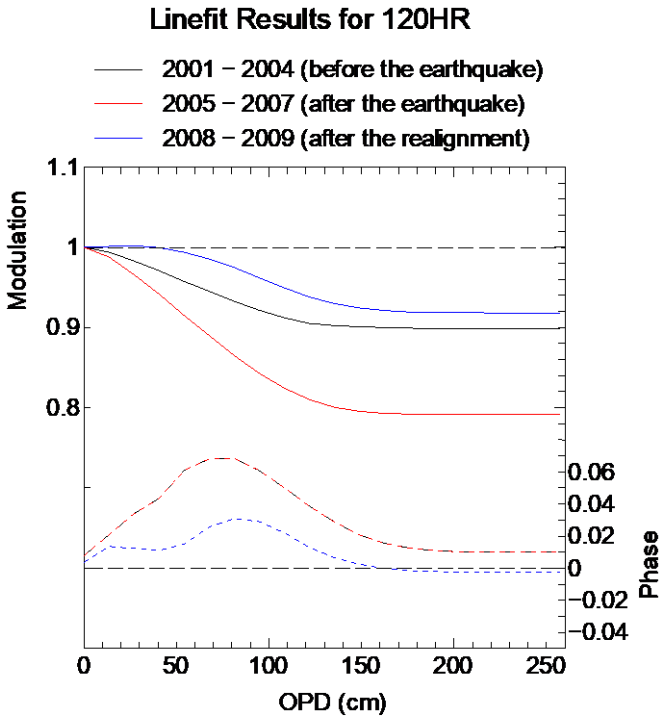


Figure 19. The modulation efficiencies and phases before and after the earthquake occurred in February 2005.

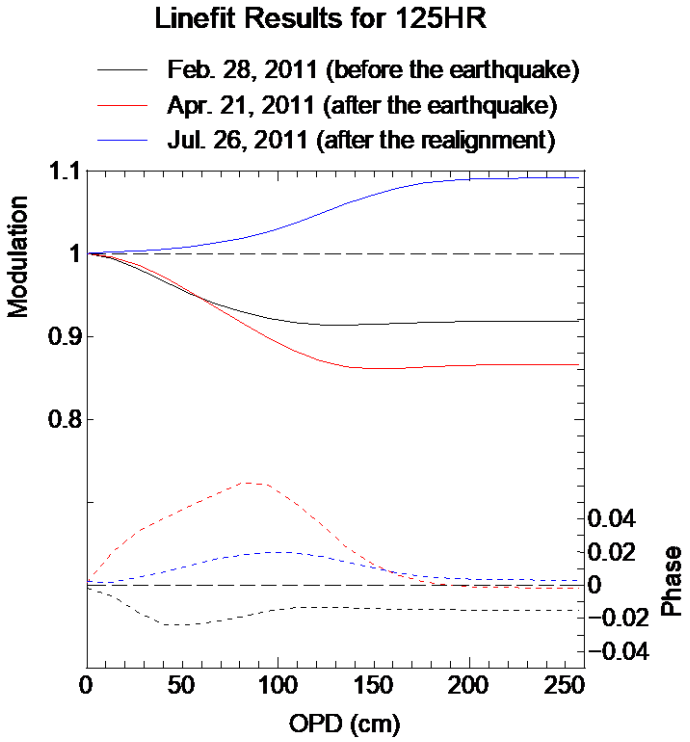


Figure 20. The modulation efficiencies and phases before and after the earthquake occurred in March 2011.

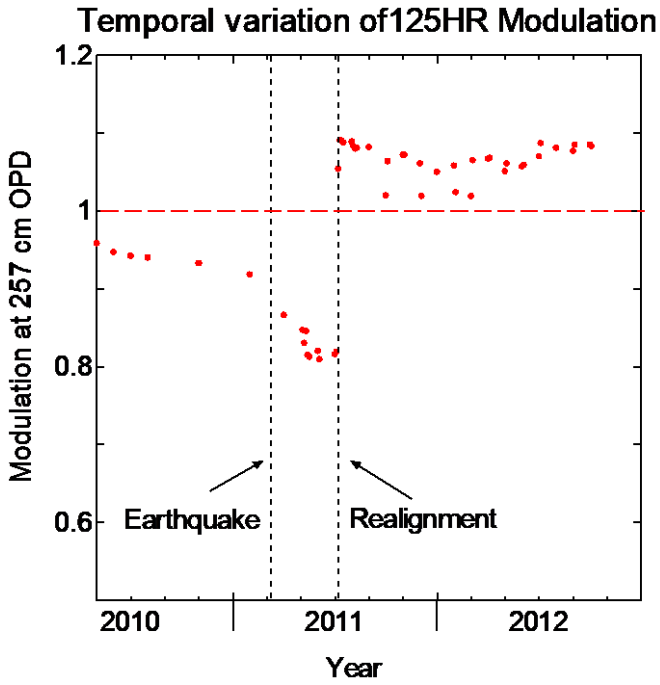

Figure 21. Temporal variation of the modulation efficiencies between 2010 and 2012 for 125HR.

**References:**

Dammers et al., Retrieval of ammonia from ground-based FTIR solar spectra, Atmos. Chem. Phys., 15, 12789–12803, 2015.

Franco et al., Retrieval of ethane from ground-based FTIR solar spectra using improved spectroscopy: Recent burden increase above Jungfraujoch, JQSRT, 160, 36-49, 2015.

Hannigan et al., Global Atmospheric OCS Trend Analysis from 22 NDACC Stations, J. Geophys. Res., Atmospheres, 127, e2021JD035764, 2022.

Sussmann et al., Strategy for high-accuracy-and-precision retrieval of atmospheric methane from the mid-infrared FTIR network, Atmos. Meas. Tech., 4, 1943–1964, 2011.

Vigouroux et al., Evaluation of tropospheric and stratospheric ozone trends over Western Europe from ground-based FTIR network observations, Atmos. Chem. Phys., 8, 6865-6886, 2008.

Vigouroux et al., Trends of ozone total columns and vertical distribution from FTIR observations at eight NDACC stations around the globe, Atmos. Chem. Phys., 15, 2915-2933, 2015.

Vigouroux et al., NDACC harmonized formaldehyde time series from 21 FTIR stations covering a wide range of column abundances, Atmos. Meas. Tech., 11, 5049–5073, 2018.